

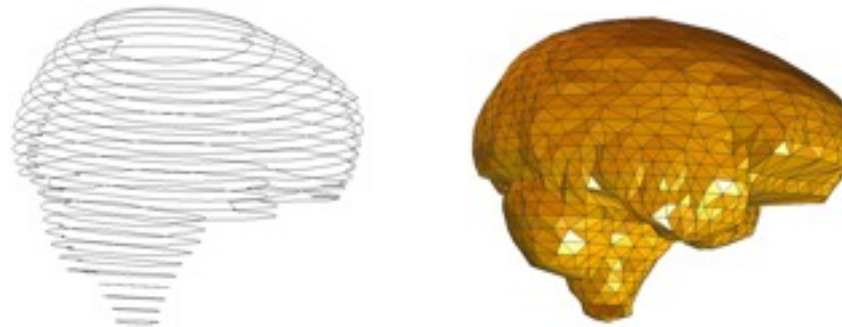
Lecture 11

CS 384R, CES 392

Geometric (Bio-) Modeling and Visualization

<http://www.cs.utexas.edu/~bajaj/cs384R2012/>

Cross-Sectional Contour Reconstruction (Surface, Volume) and Mesh Improvement



Computational Visualization Center (CVC) <http://cvcweb.ices.utexas.edu>
Dept. of Computer Science / Institute for Computational Engineering and Sciences
University of Texas at Austin

Surface Tiling Steps (revisited)

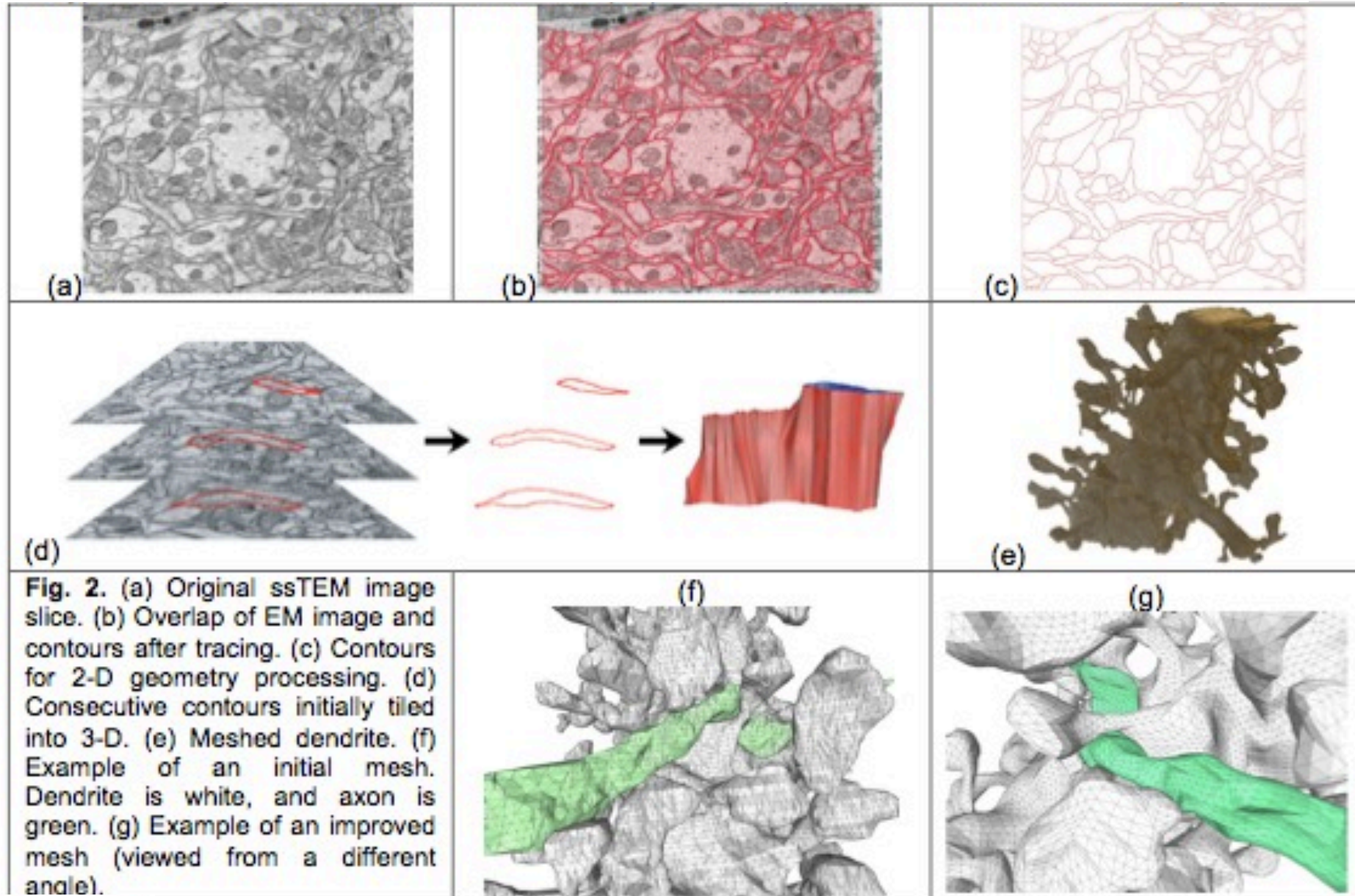


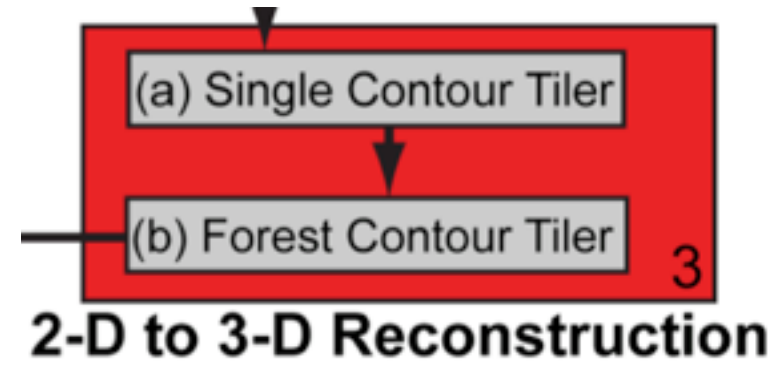
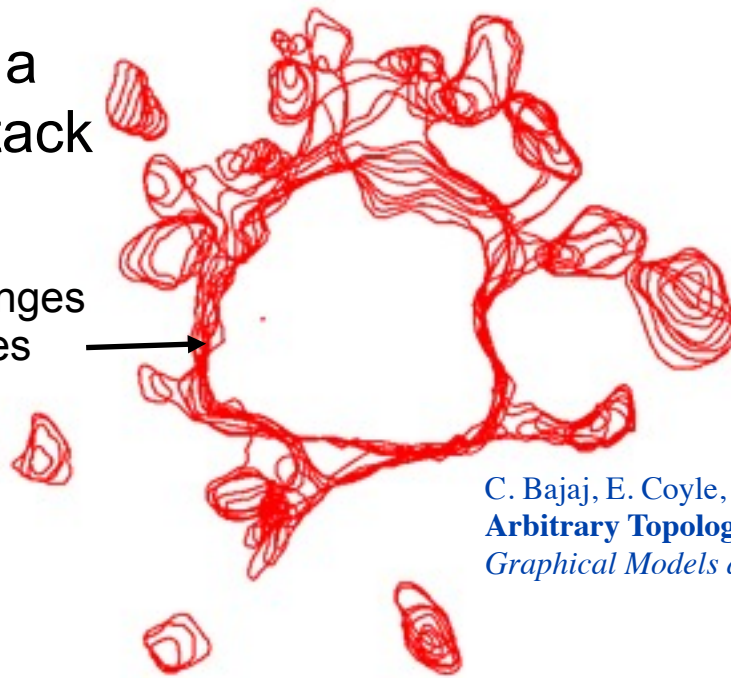
Fig. 2. (a) Original ssTEM image slice. (b) Overlap of EM image and contours after tracing. (c) Contours for 2-D geometry processing. (d) Consecutive contours initially tiled into 3-D. (e) Meshed dendrite. (f) Example of an initial mesh. Dendrite is white, and axon is green. (g) Example of an improved mesh (viewed from a different angle).



Computational Visualization Center (CVC) <http://cvcweb.ices.utexas.edu>
Dept. of Computer Science / Institute for Computational Engineering and Sciences
University of Texas at Austin

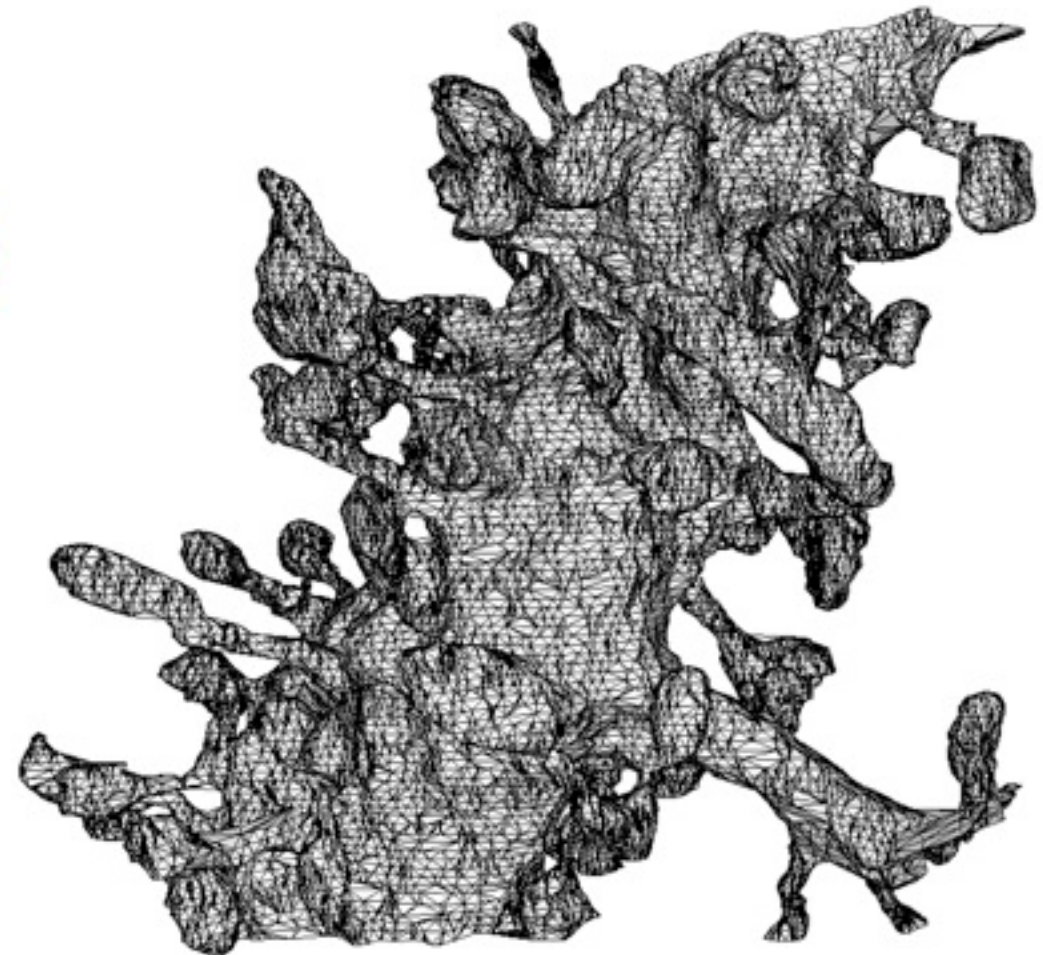
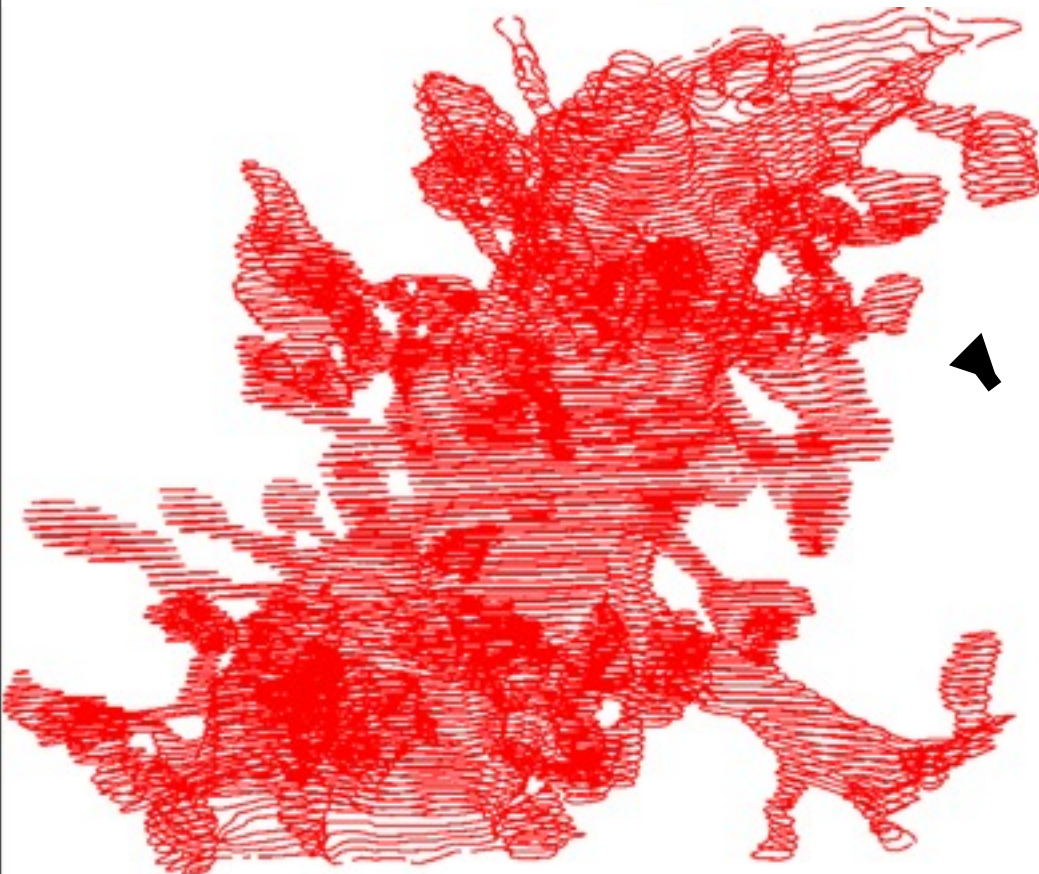
Reconstructing a Single Contour Stack

Complex Topological Changes Between Adjacent Slices

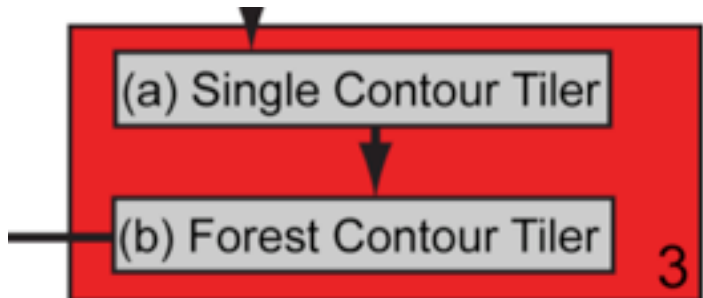


C. Bajaj, E. Coyle, K. Lin

Arbitrary Topology Shape Reconstruction from Planar Cross Sections
Graphical Models and Image Processing, 58:6, (1996), 524-543.



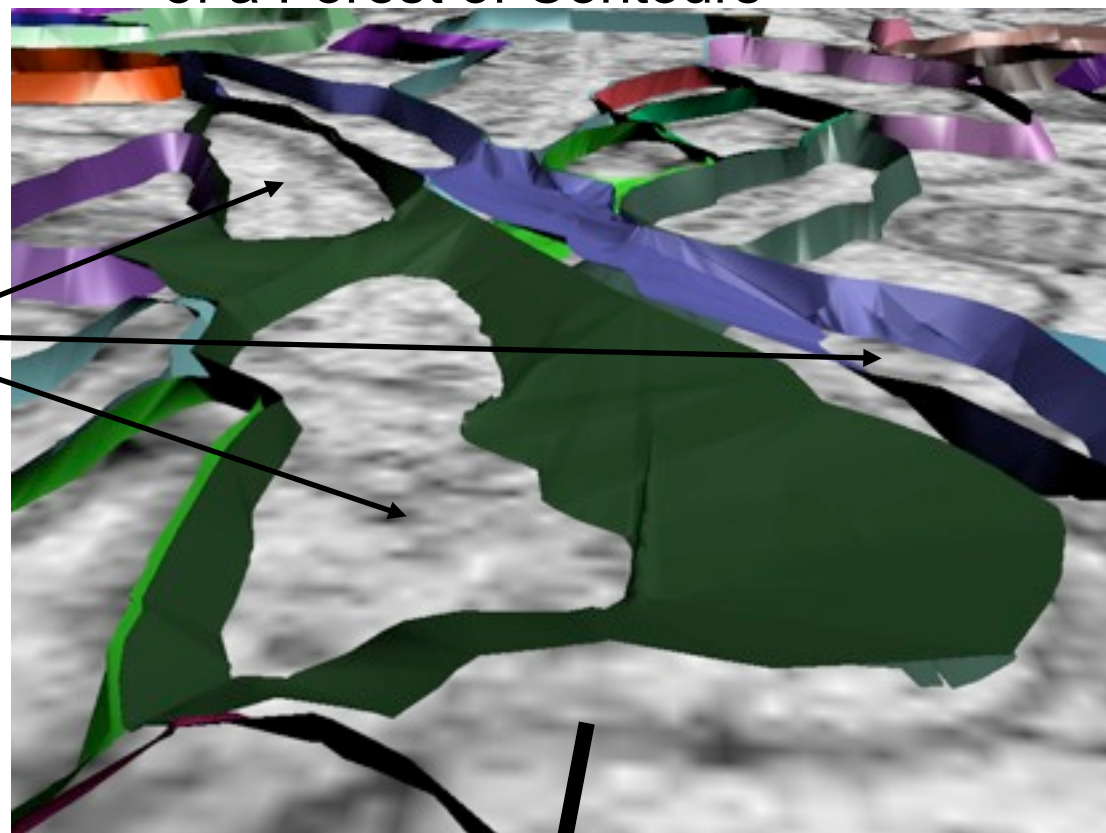
Topological/Geometric Consistent Reconstruction of a Forest of Contours



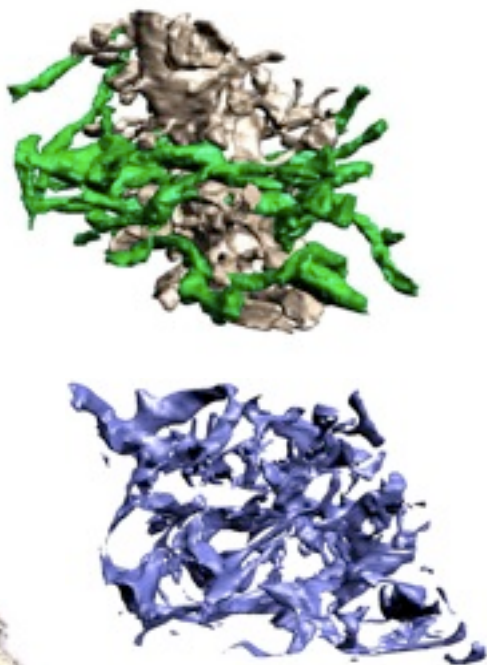
2-D to 3-D Reconstruction

Many Contours Must Be Reconstructed Simultaneously and Consistently

J. Edwards and C. Bajaj
Topologically correct reconstruction of tortuous contour forests
Computer-Aided Design, 43(10): 1296-1306, 2011

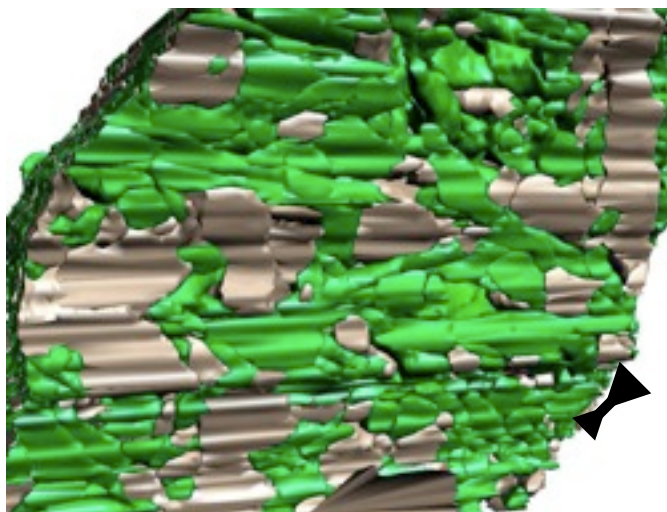


Partial Set of Reconstructed Neuronal Processes

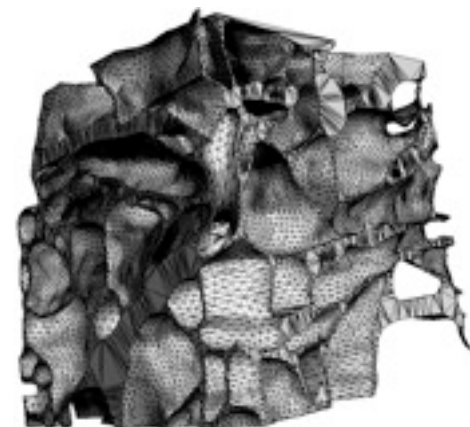


Dendrites (golden)
Axons (green)
Glial (purple)

Full Set of Reconstructed Neuronal Processes



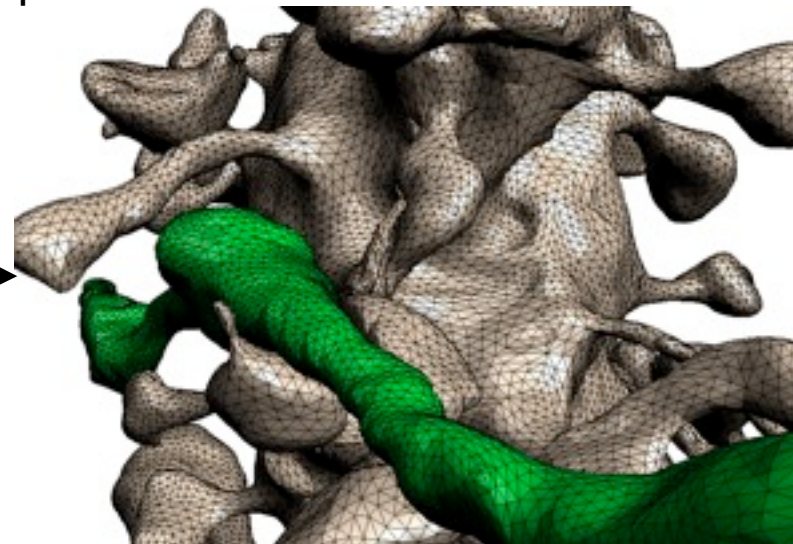
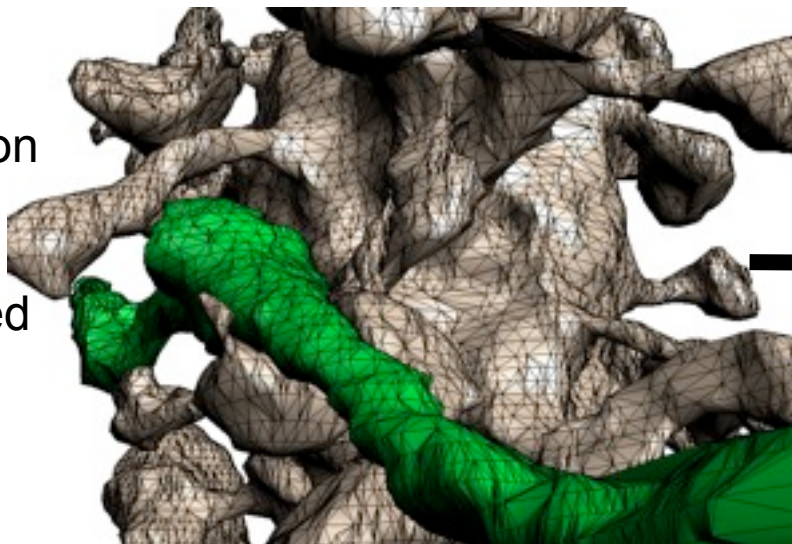
Portion of Extracellular Space



3-D Geometry Processing

Mesh Quality Improvement

Reconstruction often produces poorly-shaped triangles



C. Bajaj, E. Coyle, K. Lin

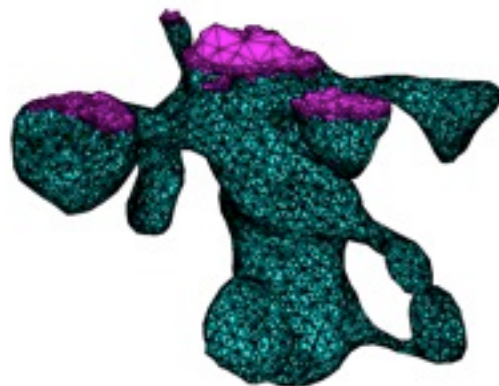
Tetrahedral Meshes from Planar Cross Sections

CMAME, 1999

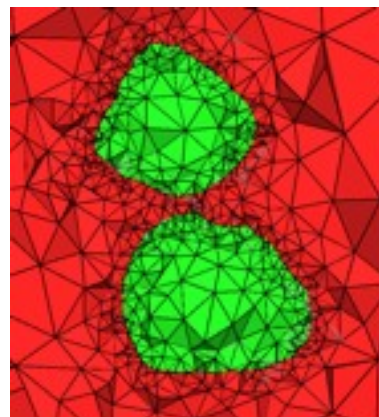
Tetrahedralization

Y. Zhang, G. Xu, C. Bajaj, **Quality Meshing with Geometric Flow** *Comm. in Numerical Methods in Engineering*, 2008.

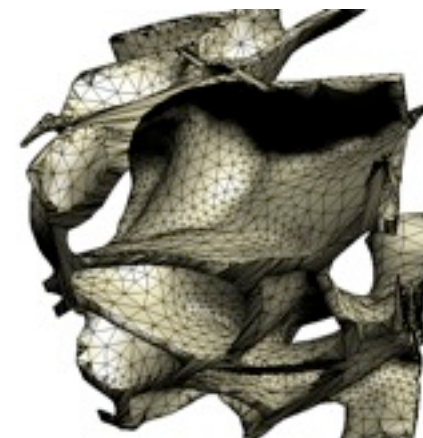
Q. Zhang, G. Xu, C. Bajaj **Quality Multi-domain meshing for Volumetric Data** *Biomed Egg & Informatics 2010*



Intra-Dendritic

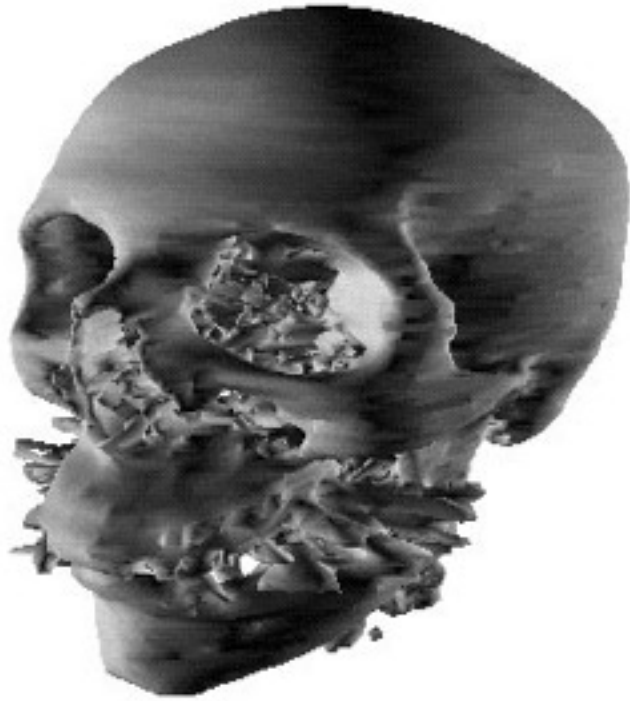


Intra & Extra-cellular

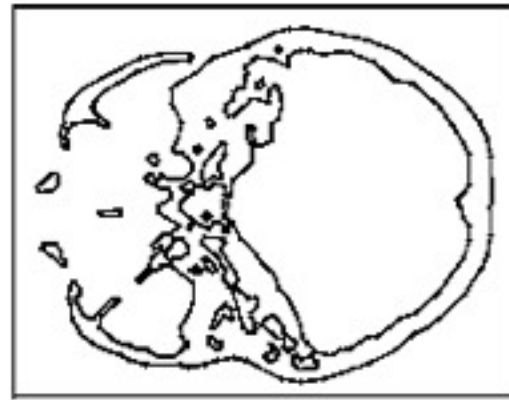


Extra-cellular

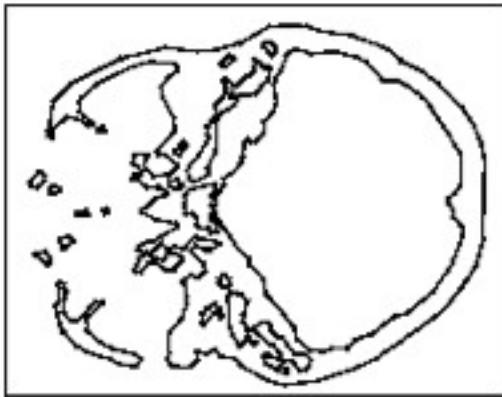
Tiling/Meshing 1



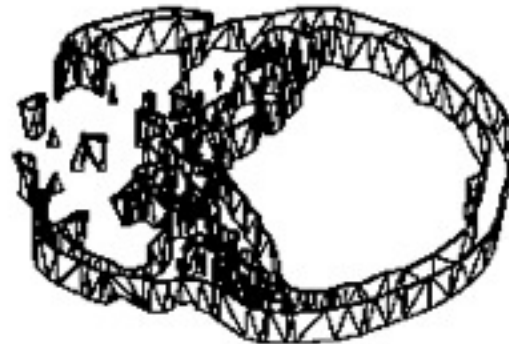
(a)



(b)



(c)

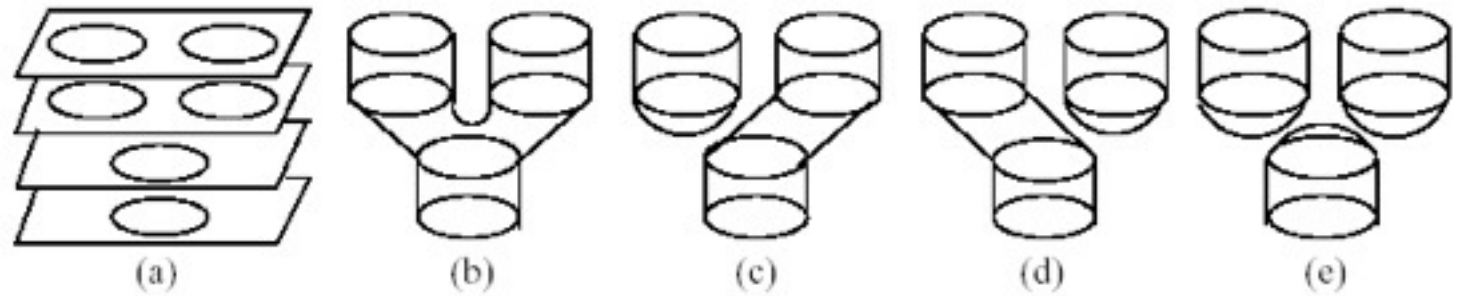


(d)

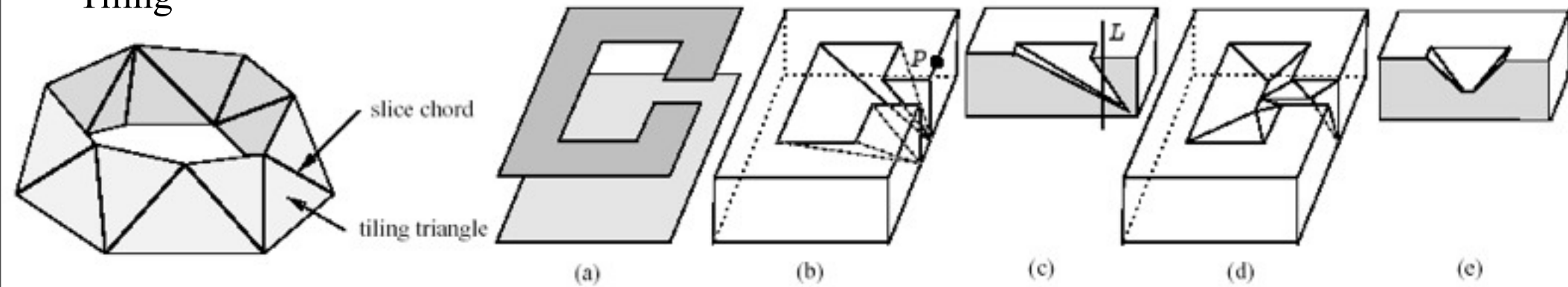
- To generate a boundary element triangular mesh from a set of cross-section polygonal slice data.
- Subproblems
 - The correspondence problem
 - The tiling problem
 - The branching problem

Sub-problems

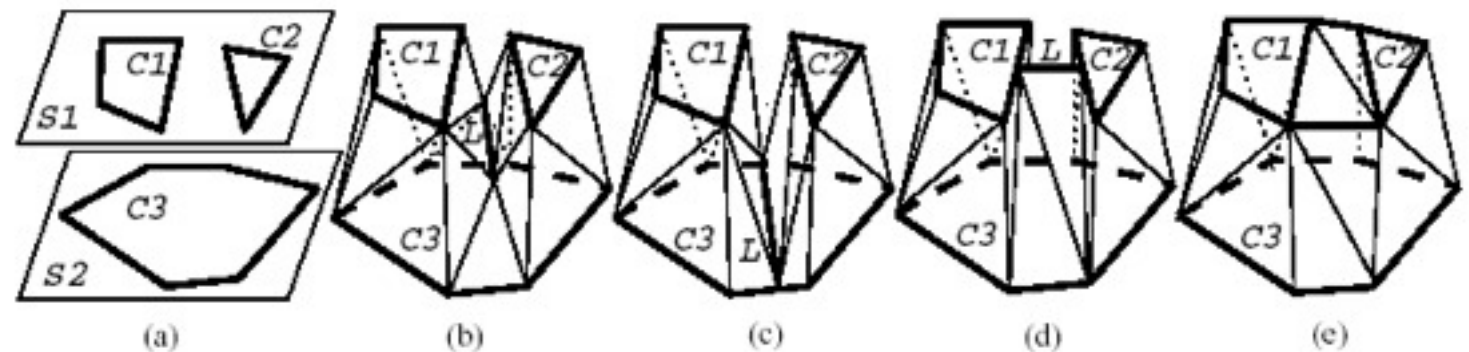
- Correspondence



- Tiling



- Branching



Criteria for Tiled (Ribbon) Mesh

Criterion 1 *The reconstructed surface and solid regions form piecewise closed surfaces of polyhedra.*

Criterion 2 *Any vertical line (a line perpendicular to the slice) between two slices intersects the reconstructed surface at zero points, one point, or along line segment (Fig. 6(a)).*

Criterion 3 *Re-sampling of the reconstructed surface on the slice should produce the original contours.*

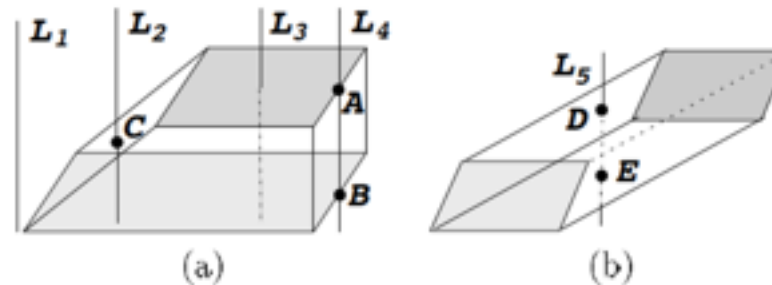
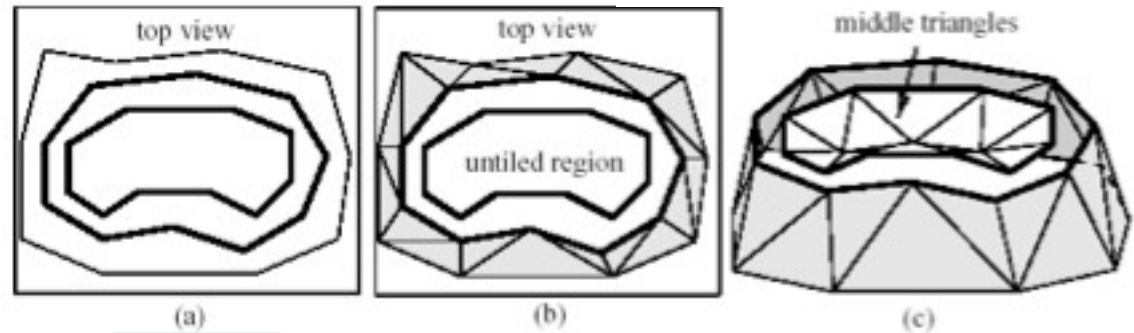
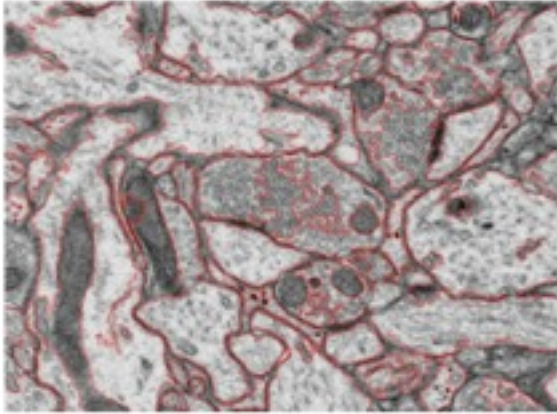


Figure 6: Criterion 2: The shaded regions are the solid regions of two slices, and the reconstructed surface is the surface covering the space between two solid regions. (a) A vertical line between two slices intersects the reconstructed surface at zero points (e.g. L_1 and L_3), one point (e.g. L_2), or one line segment (e.g. L_4). (b) The reconstructed surface shown is not allowed because the vertical line L_5 intersects the reconstructed surface at two points, D and E .

Sketch of Tiling Algorithm



Step 1: Segment closed contours from image slices.

Step 2: Create any required augmented contours.

Step 3: Find correspondences between contours.

Step 4: Form the tiling region of each vertex.

Step 5: Construct the tiling.

Step 6: Collect the boundaries of untilted regions.

Step 7: Form triangles to cover untilted regions based on their edge Voronoi diagram (EVD).

C. Bajaj, E. Coyle, K. Lin

Arbitrary Topology Shape Reconstruction from Planar Cross Sections

Graphical Models and Image Processing, 58:6, (1996), 524-543.

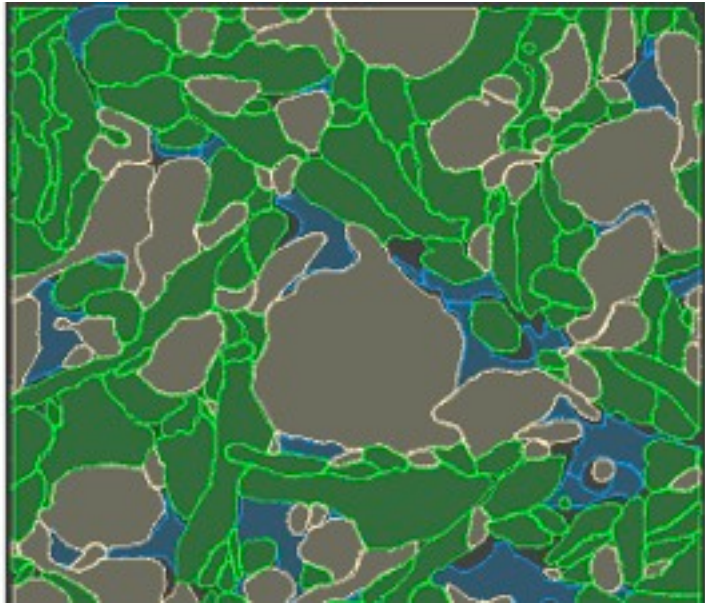
Computational Visualization Center (CVC) <http://cvcweb.ices.utexas.edu>

Dept. of Computer Science / Institute for Computational Engineering and Sciences

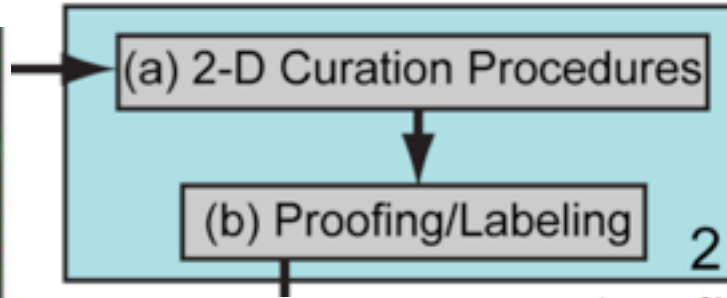
University of Texas at Austin



Steps 1&2



2-D Geometry Processing

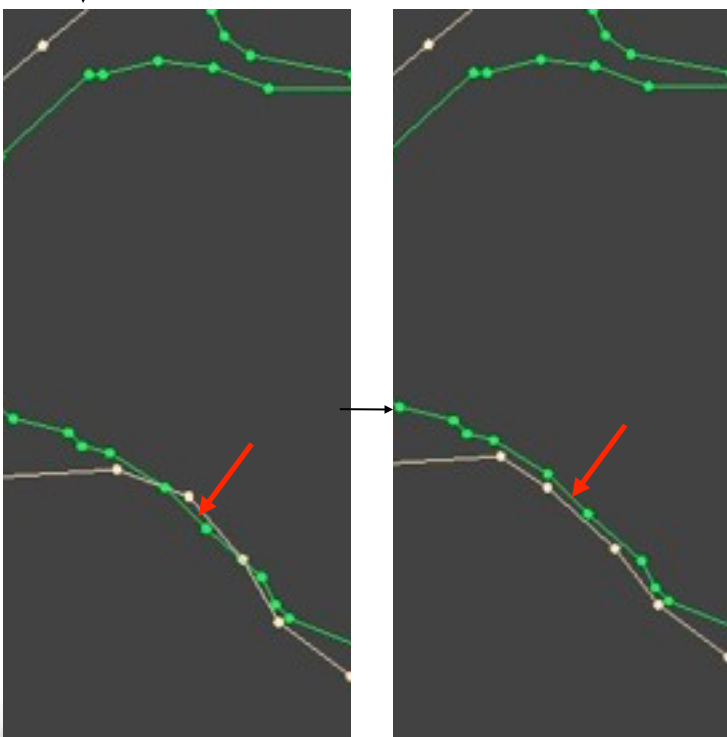


Spline-Fitted Contours

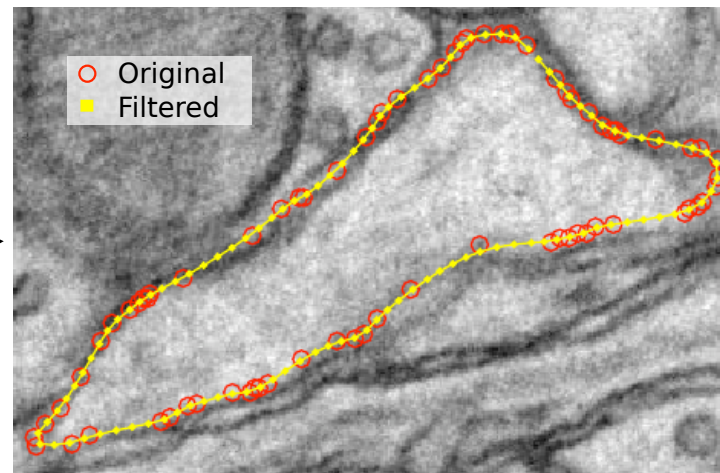


Traced Contours

2D Curation



Contour Resampling



C. Bajaj, G. Xu, Q. Zhang

A Fast Variational Method for the Construction of Adaptive Resolution C^2 Smooth Surfaces

CMAME, (2009)



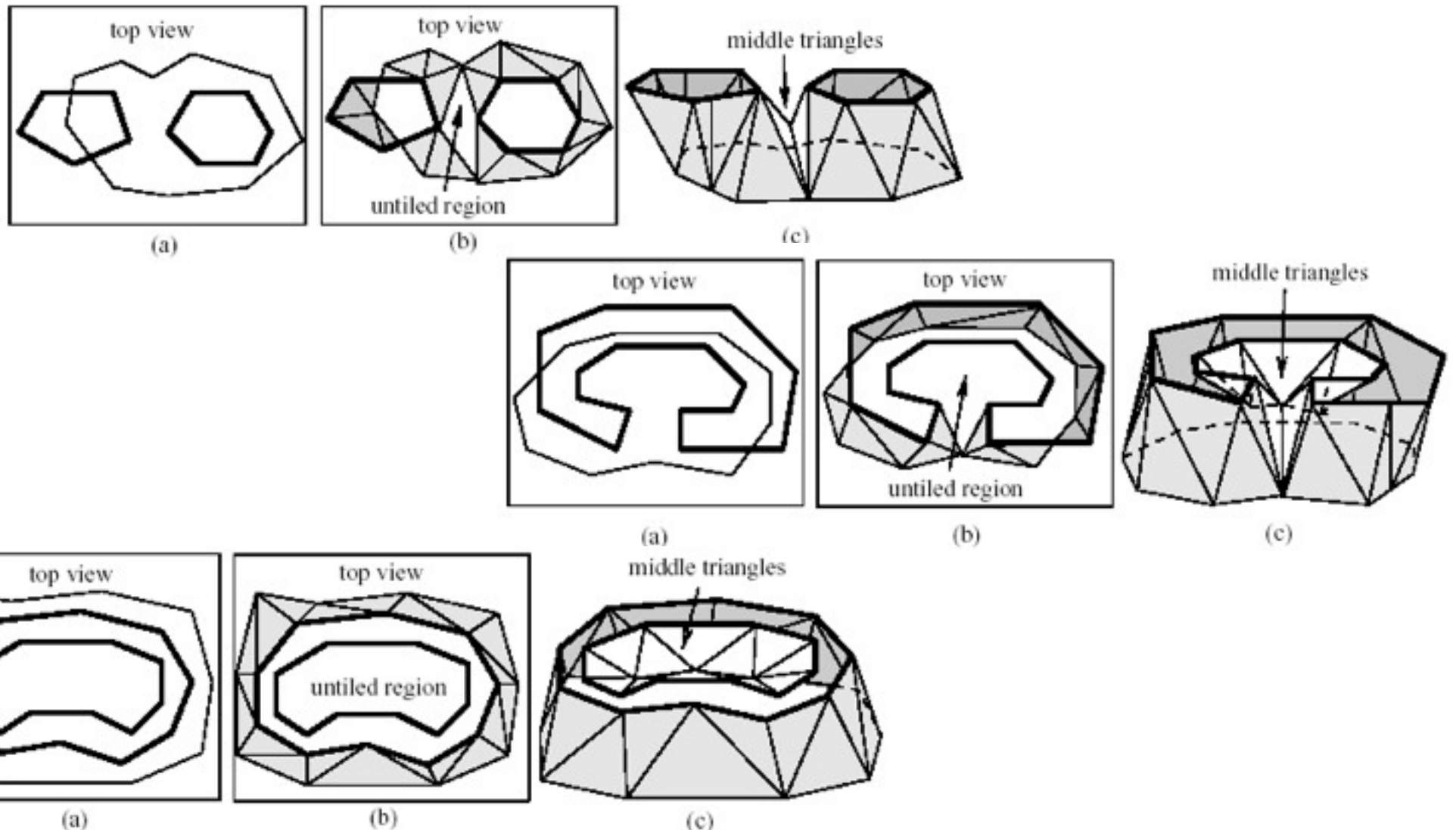
C. Bajaj, A. Gillette, S. Goswami

Topology Based Selection and Curation of Level Sets

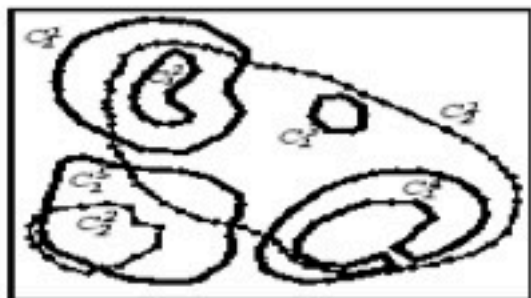
Topology-in-Visualization, ed. by A. Wiebel, H. Hege, K. Polthier, G. Scheuermann, 2009

Tiling Steps 3 - 6

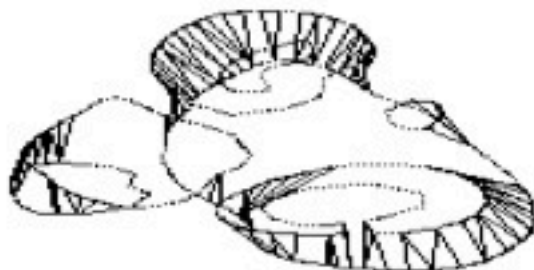
- A multi-pass tiling approach followed by the postprocessing of untilted regions



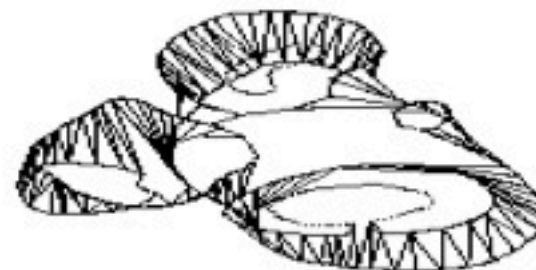
UnTiled Regions for Real Data



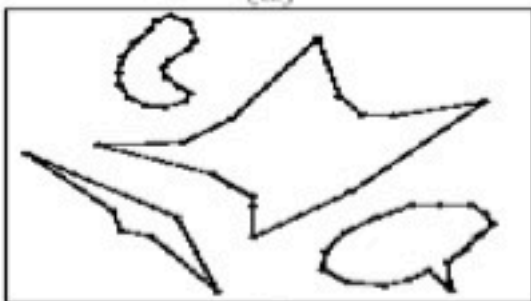
(a)



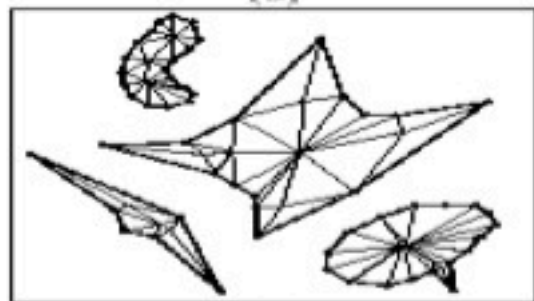
(b)



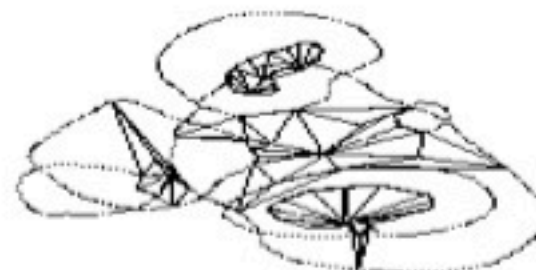
(c)



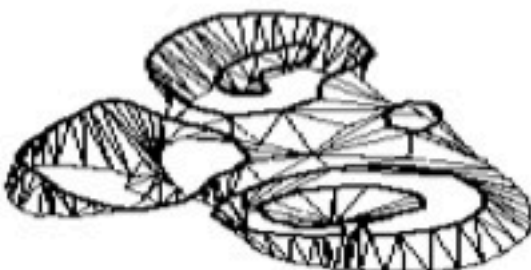
(d)



(e)



(f)



(g)



(h)



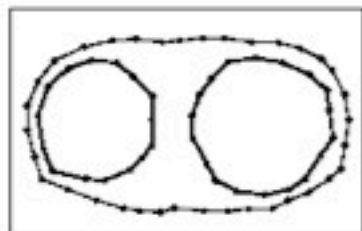
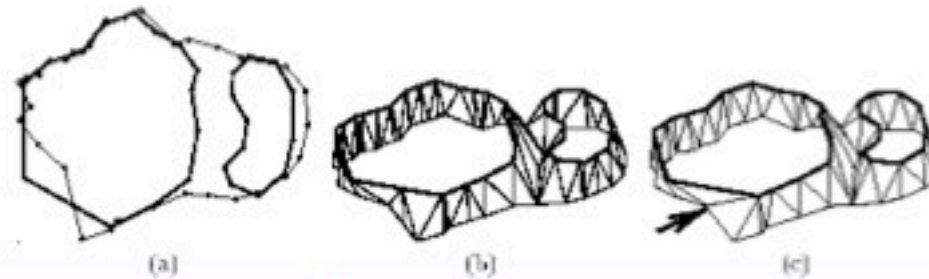
(i)



Computational Visualization Center (CVC) <http://cvcweb.ices.utexas.edu>
Dept. of Computer Science / Institute for Computational Engineering and Sciences
University of Texas at Austin

Processing Un-Tiled Regions with Branching

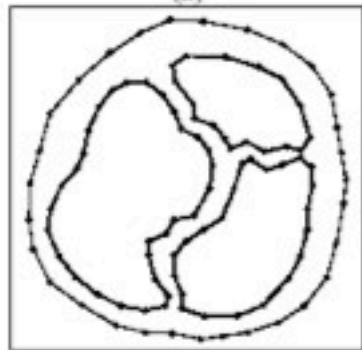
Using the Edge Voronoi Diagram as Ridges



(a)



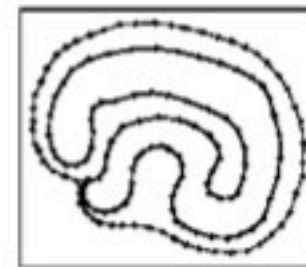
(b)



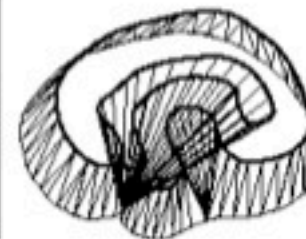
(c)



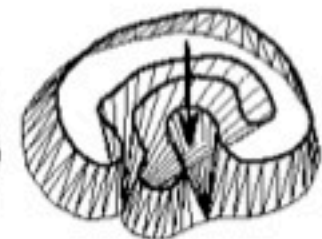
(d)



(a)



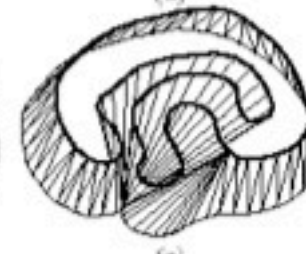
(b)



(c)



(d)



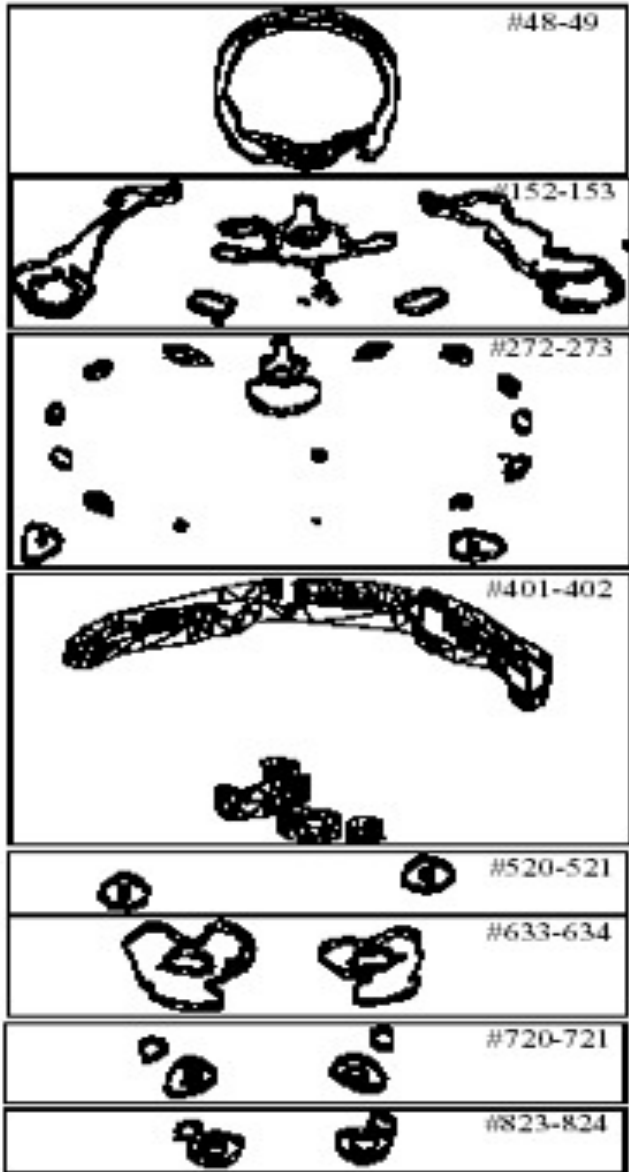
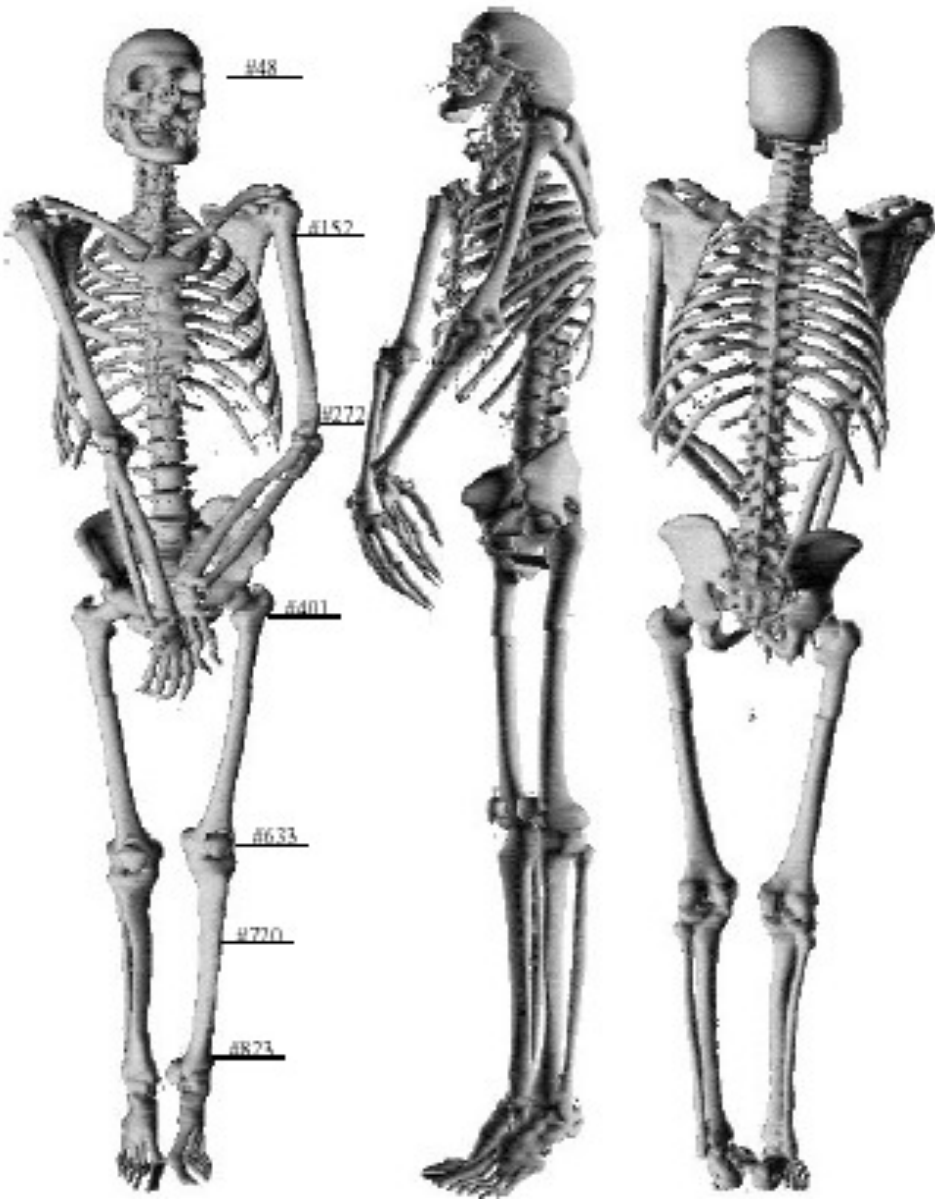
(e)



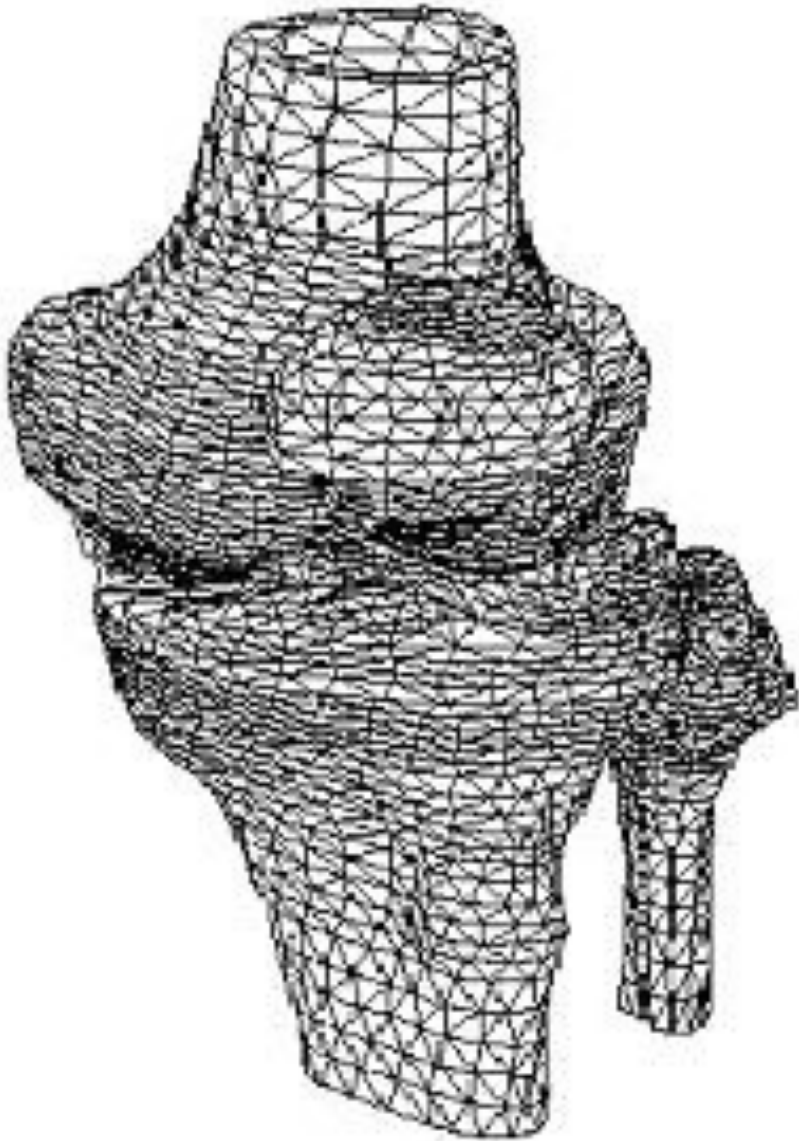
(f)



Boundary Element Triangular Mesh



Meshing II



- To generate a 3D finite element tetrahedral mesh of the simplicial polyhedron obtained via the BEM construction of cross-section polygonal slice data.
- Subproblems
 - The shelling of tetrahedra to reduce polyhedron to prisms
 - The tetrahedralization of prisms

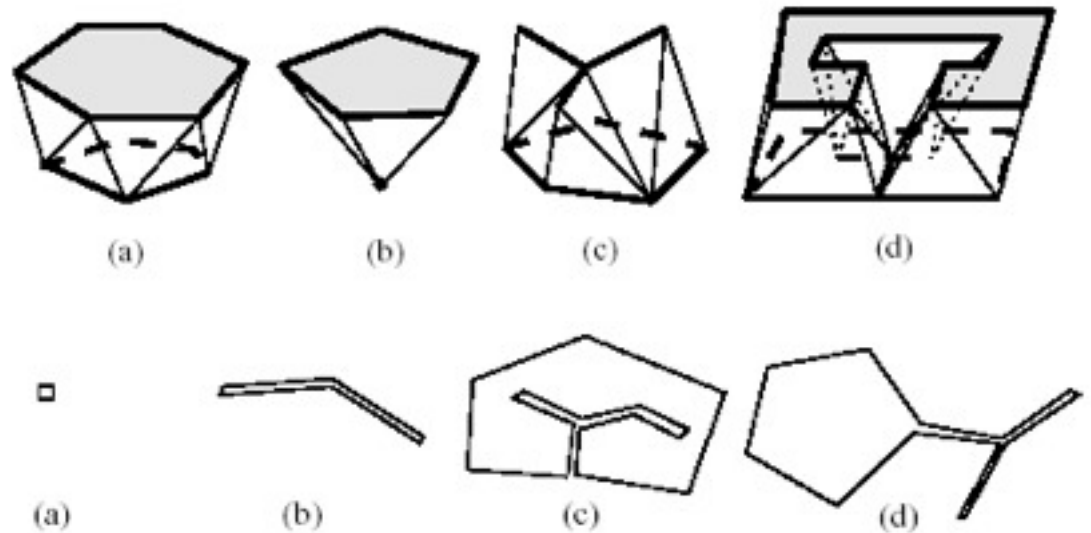
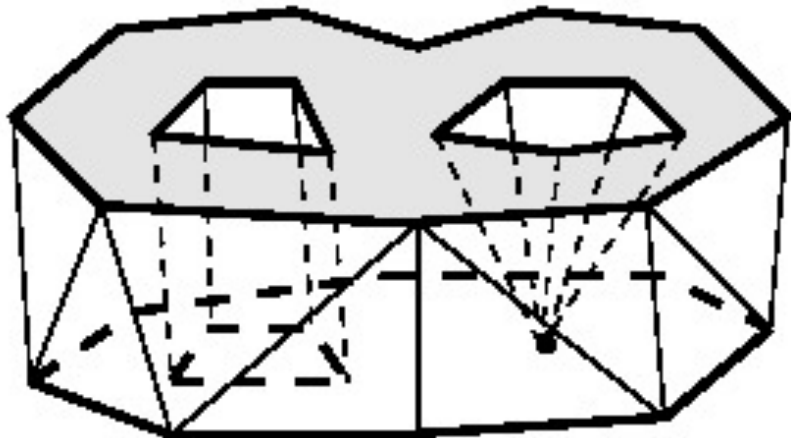
C. Bajaj, E. Coyle, K. Lin

Tetrahedral Meshes from Planar Cross Sections

CMAME, 1999

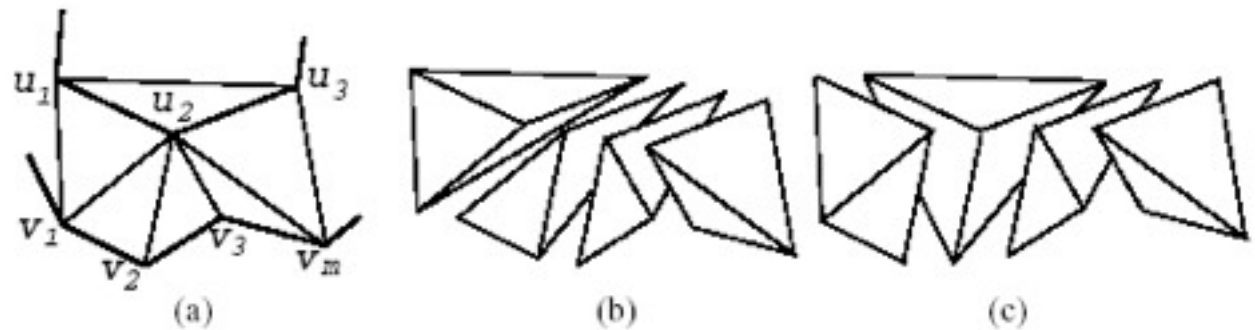
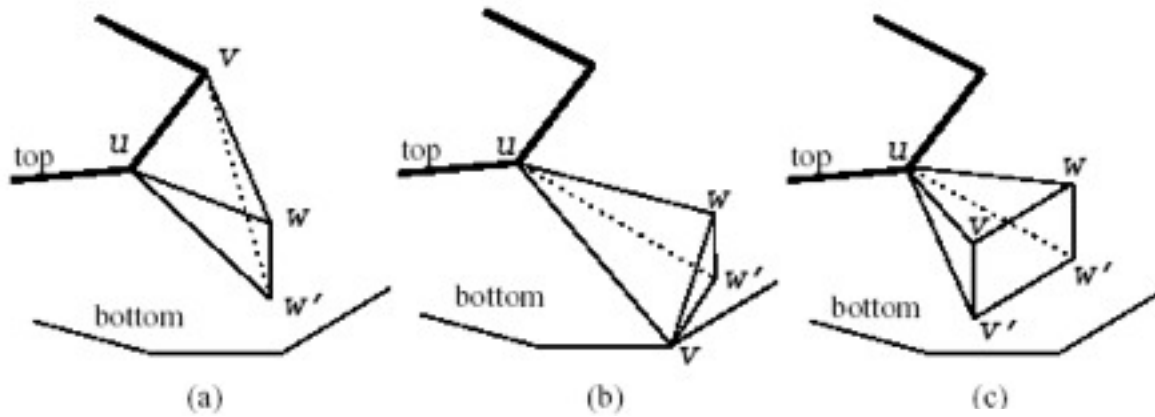
What is prismatoid?

A prismatoid is a polyhedron having for bases two polygons in parallel planes, and for lateral faces triangles or trapezoids with one side lying in one base, and the opposite vertex or side lying in the other base, of the polyhedron.



The Shelling Step

- Shell tetrahedra from the polyhedron, so the remaining part is a prismaticoid or can be divided into prismaticoids.



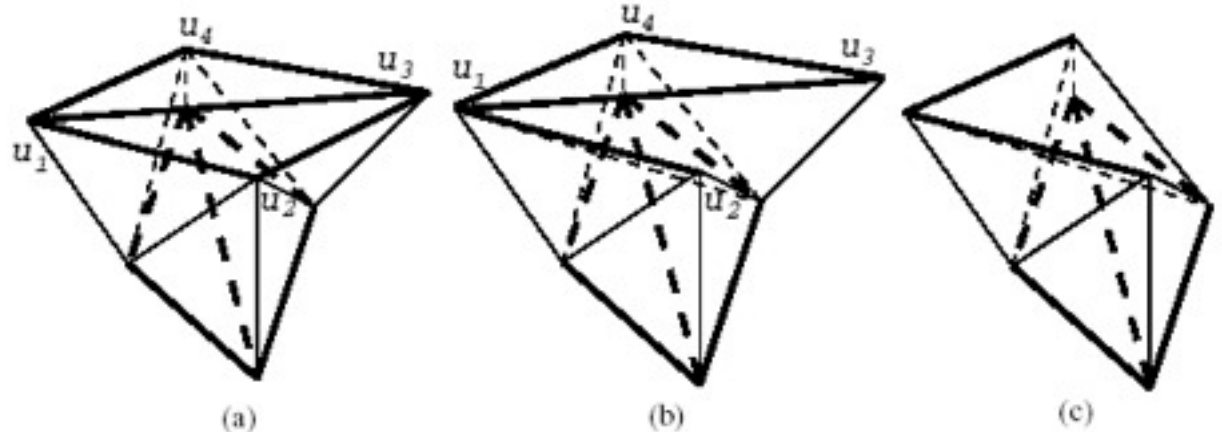
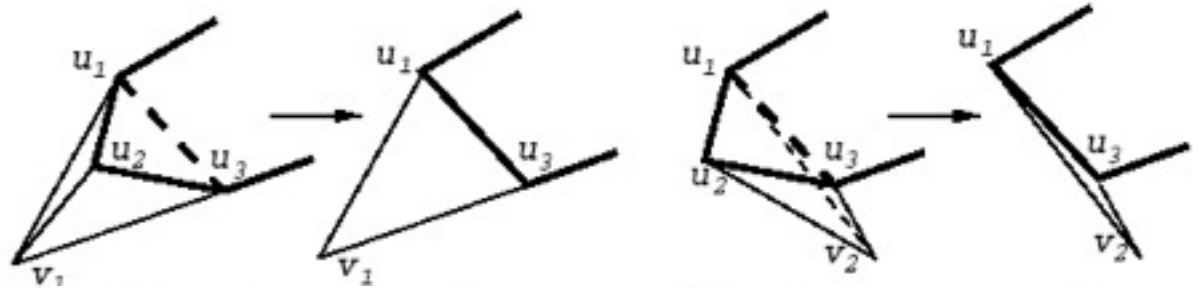
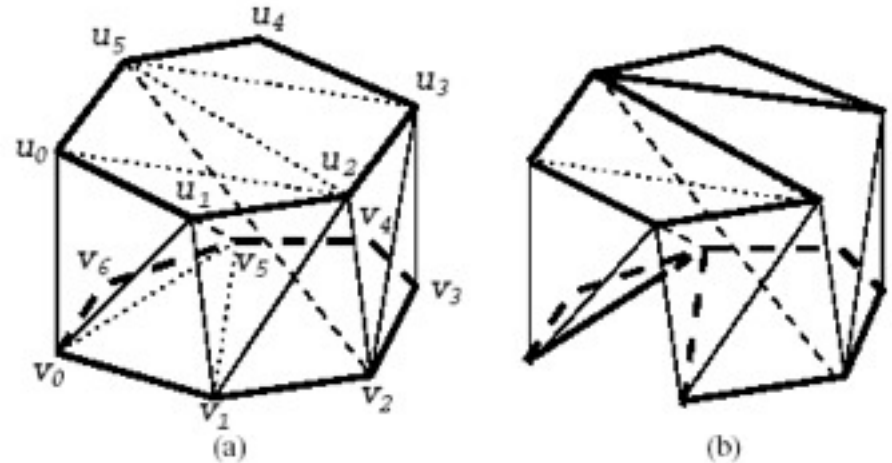
Prismatoid \rightarrow Tetrahedra

- To tetrahedralize a non-nested prismatoid without Steiner points.
 1. For each boundary triangle on both slices, calculate its metric.
 2. Pick up the boundary triangle with the best metric and form one set of tetrahedra.
 3. Update the advancing front and go to Step 1.
 4. If the remaining part is non-tetrahedralizable, backtrack and select another choice in Step 1.

Metric, Weight Factor, Grouping

- Metric = volume/(edge)³
- Weight factor

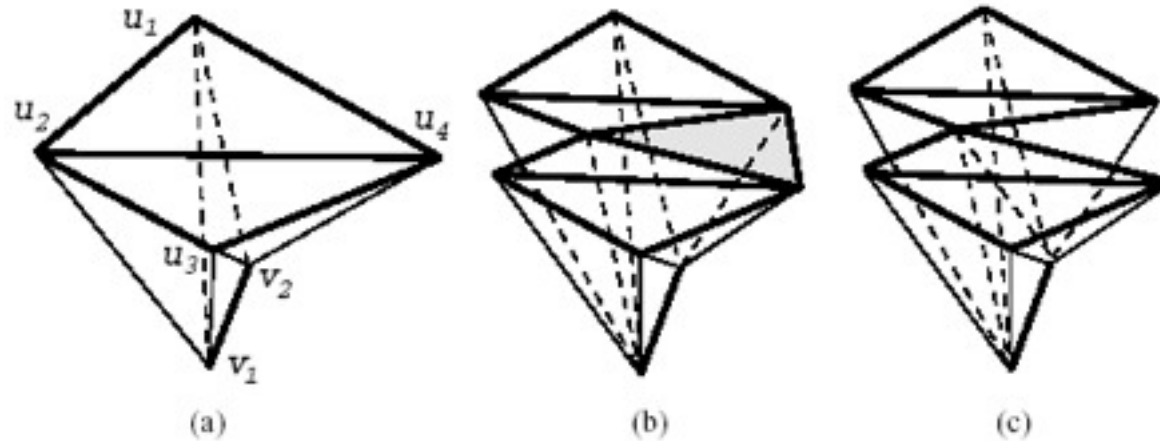
$$w = \begin{cases} 2(1 - \frac{d}{h}) & \text{if } d \leq 0.5h \\ 1 & \text{if } 0.5h < d < h \\ \frac{h}{d} & \text{if } d \geq h \end{cases}$$



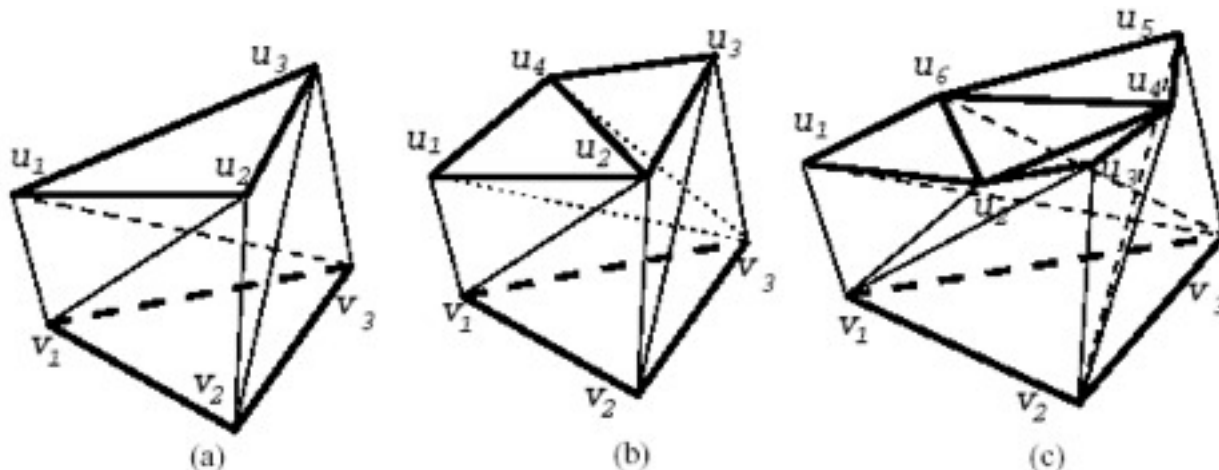
- Grouping can avoid irregular remaining part

Classification of Untetrahedralizable Prismatoids

1. Has two boundary triangles on the top face and one line segment on the bottom face.



2. Has one bottom triangle which is treated as three boundary triangles.

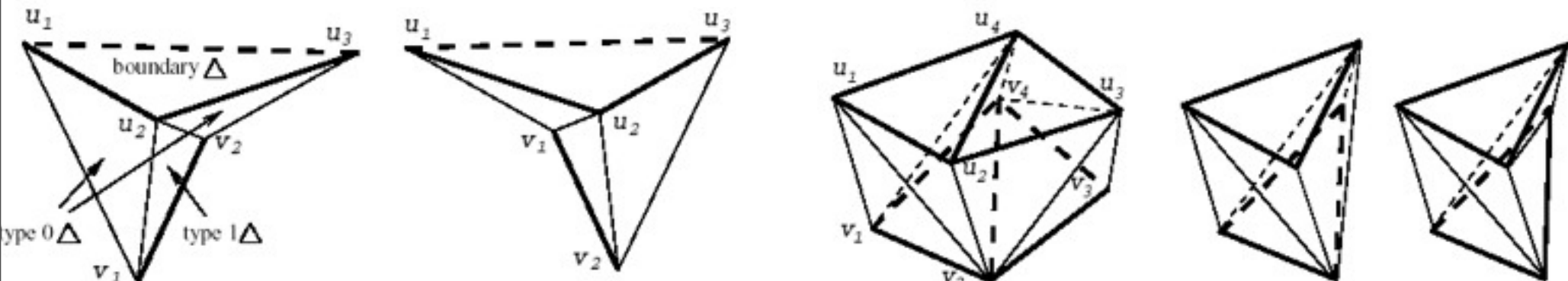


Schonhardt

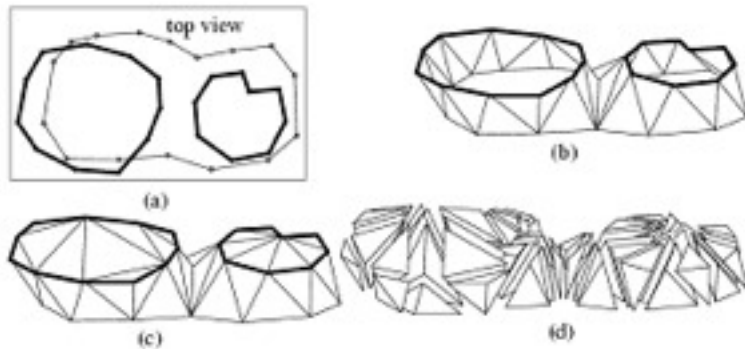
Protection Rules

Lemma 1: Suppose a top boundary triangle $\Delta u_1 u_2 u_3$ is under the constraint that no more than one type 1 triangle is between the two type 0 triangles containing the contour segments $u_1 u_2$ and $u_2 u_3$. Furthermore, let the bottom vertices of the two type 0 triangles be v_1 and v_2 . Our grouping operation cannot apply to $\Delta u_1 u_2 u_3$ to form a set of tetrahedra, if and only if all the following conditions are satisfied.

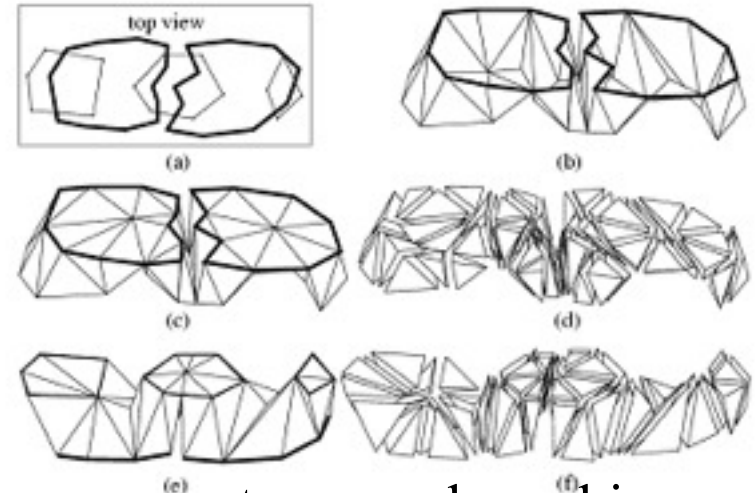
1. $v_1 v_2$ is exactly one contour segment.
2. One of the slice chords $u_2 v_1$ and $u_2 v_2$ is reflex and the other is convex.
3. Both $u_1 v_2$ and $u_3 v_1$ are not inside the prismatoid.



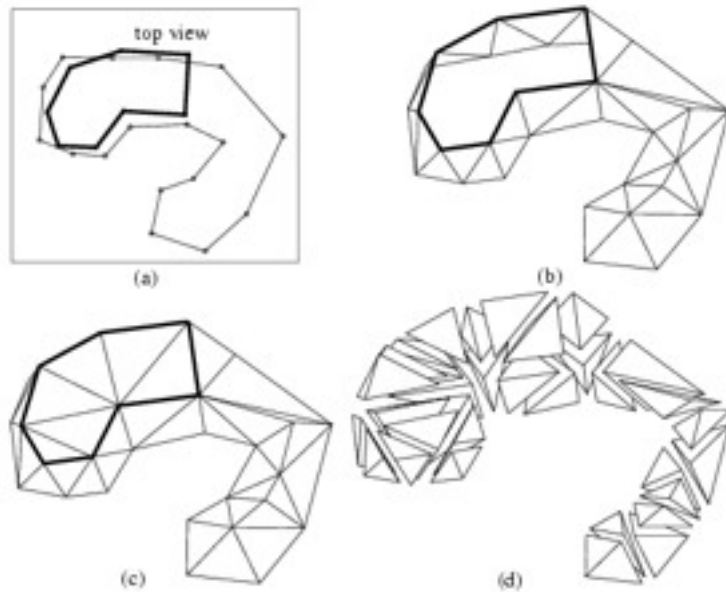
Multiple Tetrahedralizable Cases



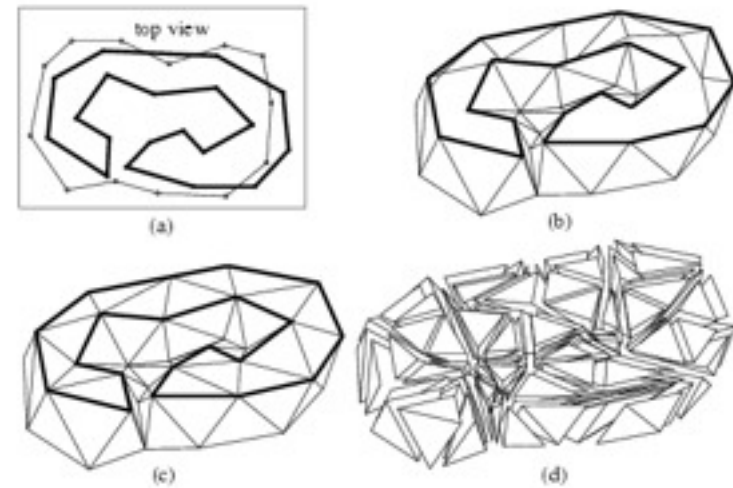
One-to-many branching



many-to-many branching

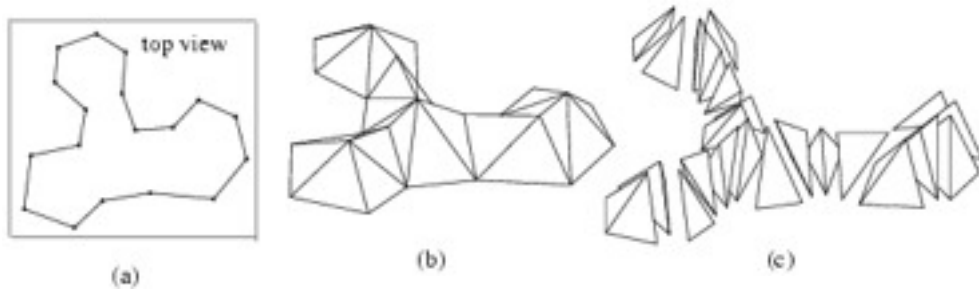


Dissimilar region (the right bottom portion of the bottom contour)

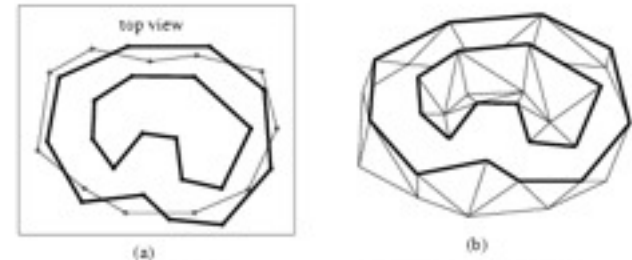


Dissimilar region (the inner portion of the top contour)

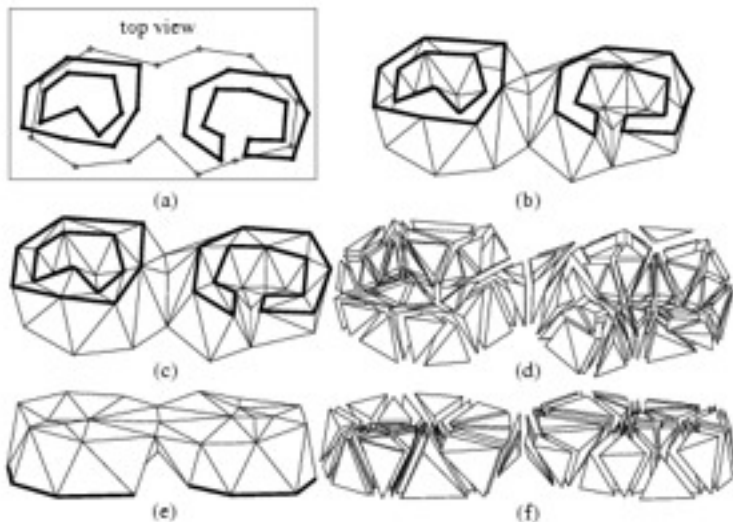
Multiple Tetrahedralizable Cases



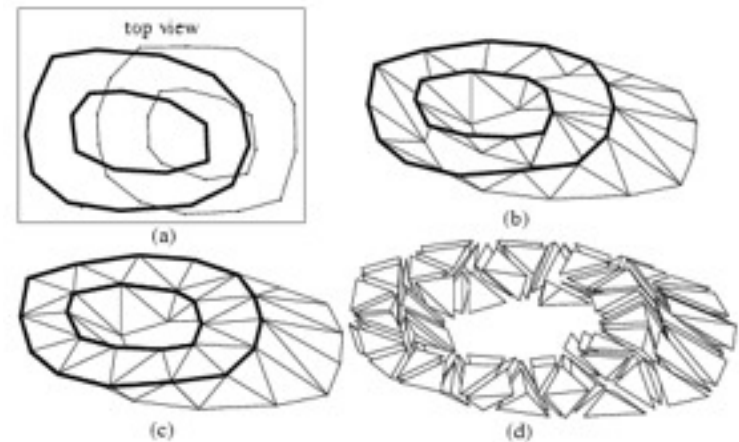
(a) (b) (c)
 Appearing/disappearing vertical feature of a solid interior



(a) (b)
 (c) (d)
 Appearing/disappearing vertical feature (the top inner contour) of a void interior

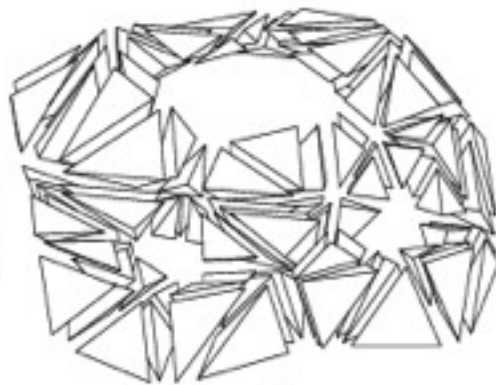
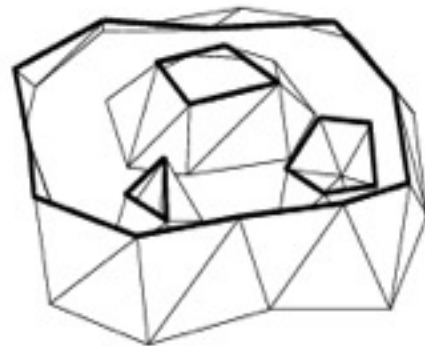
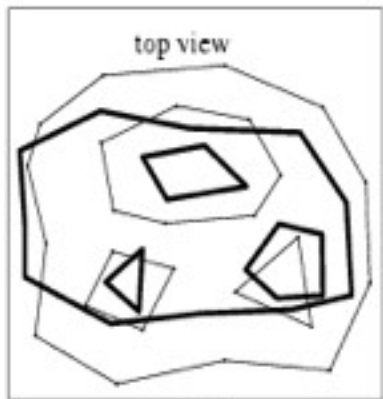


(a) (b)
 (c) (d)
 (e) (f)
 A branching, a dissimilar portion (the inner portion of the top right contour), and an appearing/disappearing vertical feature (the inner contour at the left of the top slice)

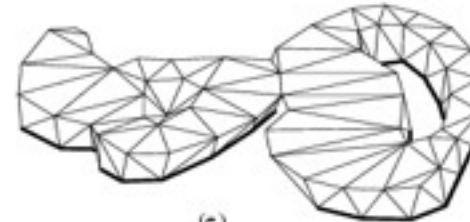
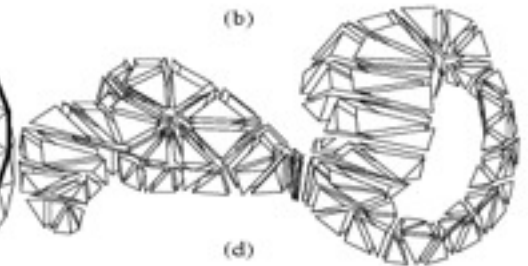
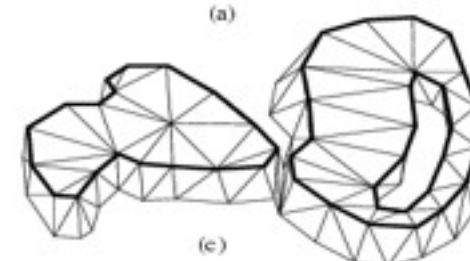
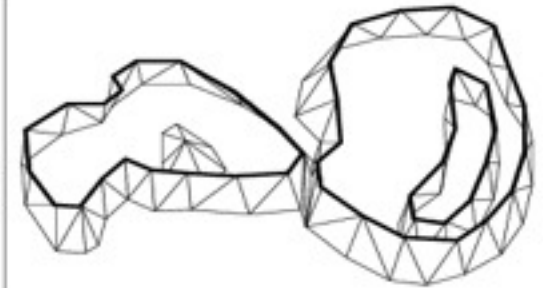
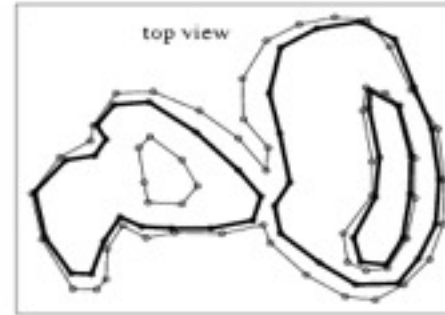


(a) (b)
 (c) (d)
 Nested prisms

Multiple Tetrahedralizable Cases

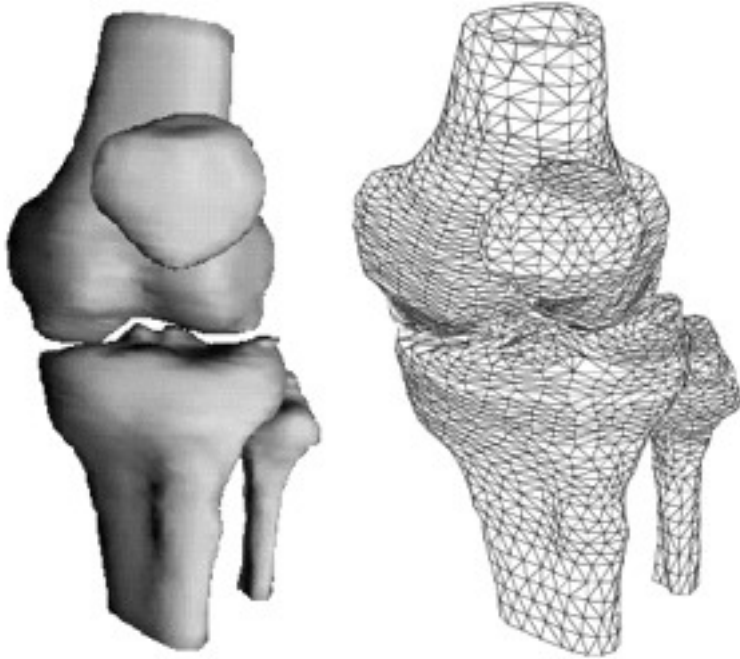


Multiply-nested prismatic solid



Solid region between two slices
of a human tibia

Examples



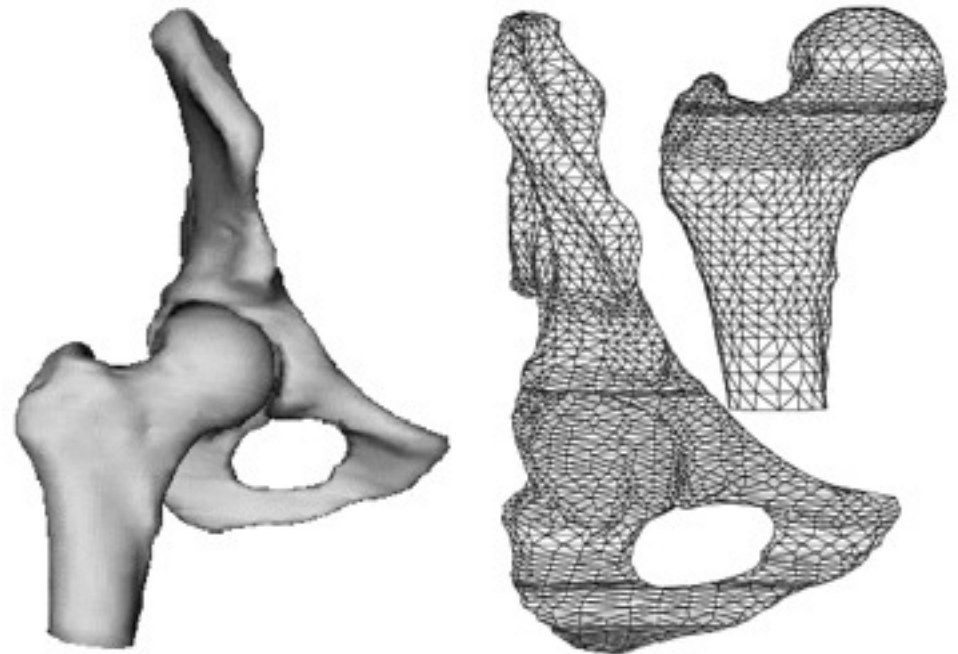
(a)

(b)

Knee joint (the lower femur, the upper tibia and fibula and the patella)

(a) Gouraud shaded

(b) The tetrahedralization



(a)

(b)

Hip joint (the upper femur and the pelvic joint)

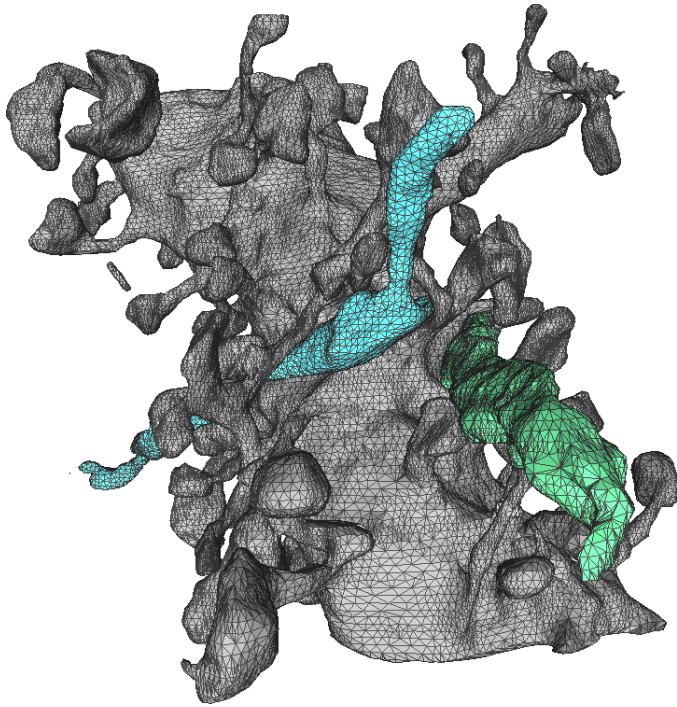
(a) Gouraud shaded

(b) The tetrahedralization

Mini-summary

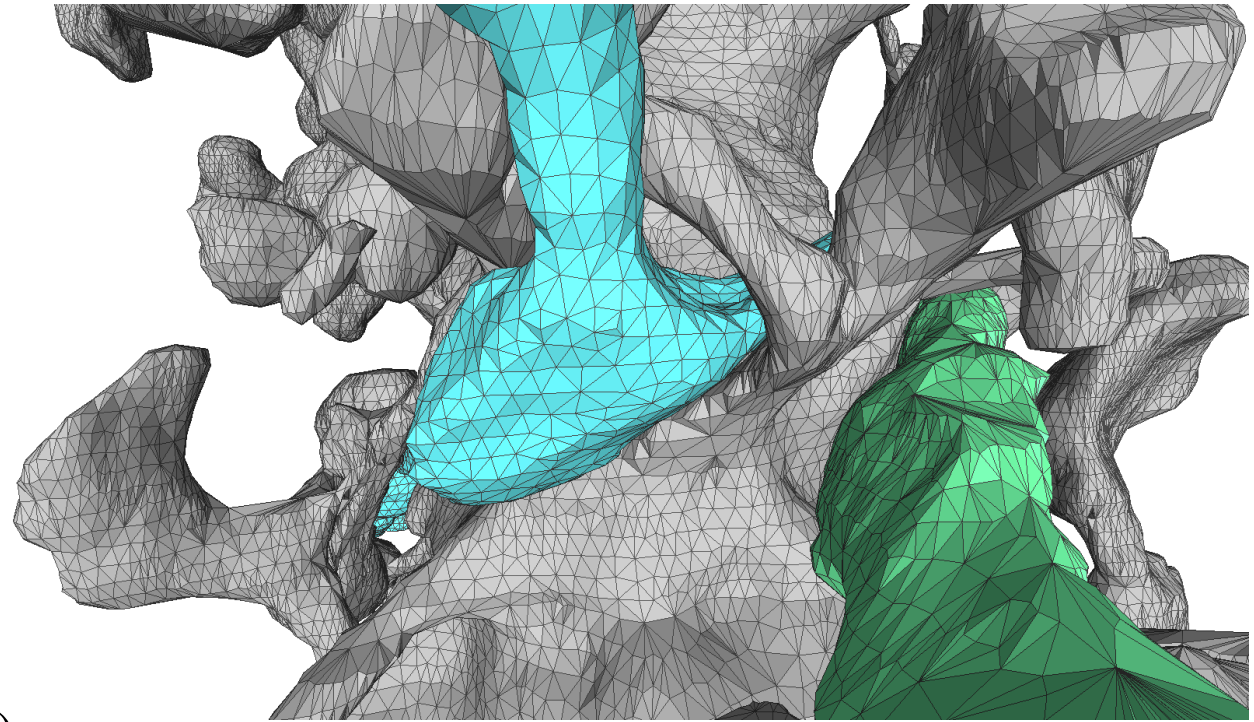
- The characterization, avoidance of non-tetrahedralizable polyhedra is one of the main challenges
- The mix of numerical precision and topological decision making needs precise rules so errors don't propagate.

Decimation & Mesh Improvement



(a)

Decimation



(b)

Mesh Quality Improvement

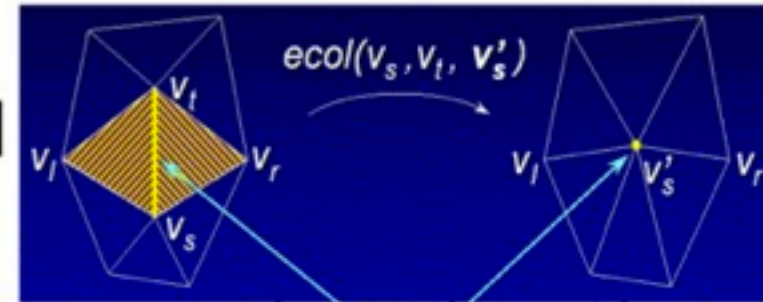


Computational Visualization Center (CVC) <http://cvcweb.ices.utexas.edu>
Dept. of Computer Science / Institute for Computational Engineering and Sciences
University of Texas at Austin

Decimation Techniques

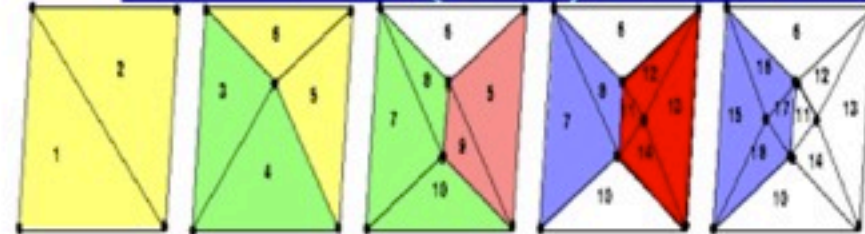
✳ Edge Contraction

[Hoppe96] [Popovic,Hoppe97] [Stadt,Gross98]
[Trotts,Hamann,Joy,Wiley98][Gueziec96]



✳ Vertex Removal

[Bajaj,Schikore98][De Berg,Dobrindt98]
[Lee,Dobkin,Sweldens,Cowsar,Schroder98]



✳ Triangle Contraction

[Hamann97]

✳ Hole Re-triangulation

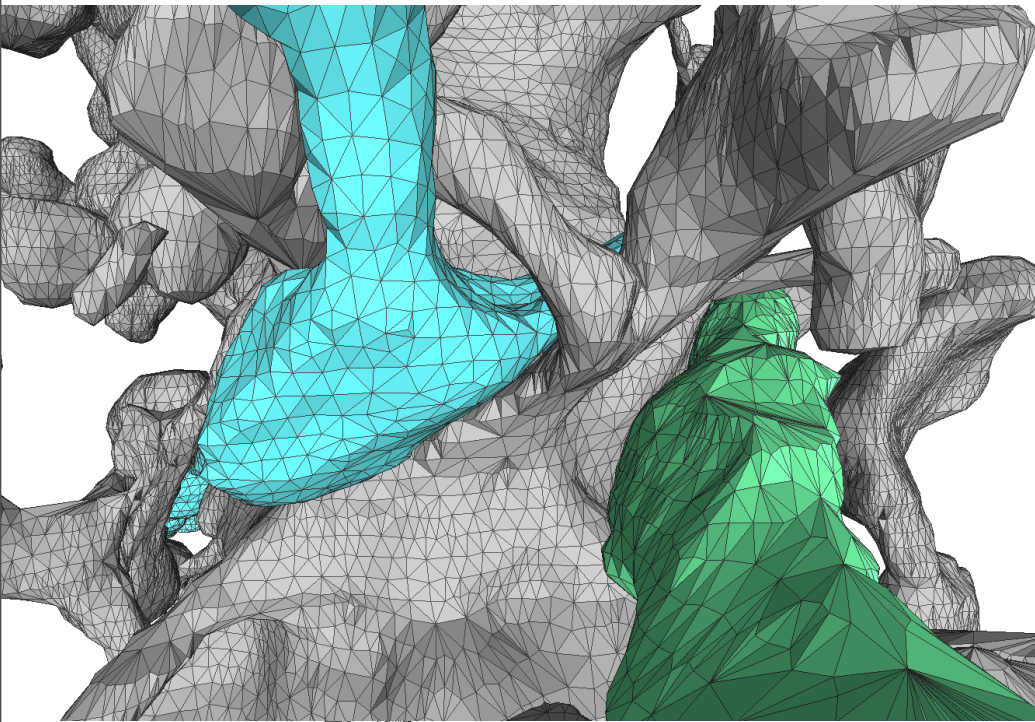
[Defloriani89] [Cohen,Varshney,Manocha,Turk96]

✳ General Re-triangulation [Turk92]

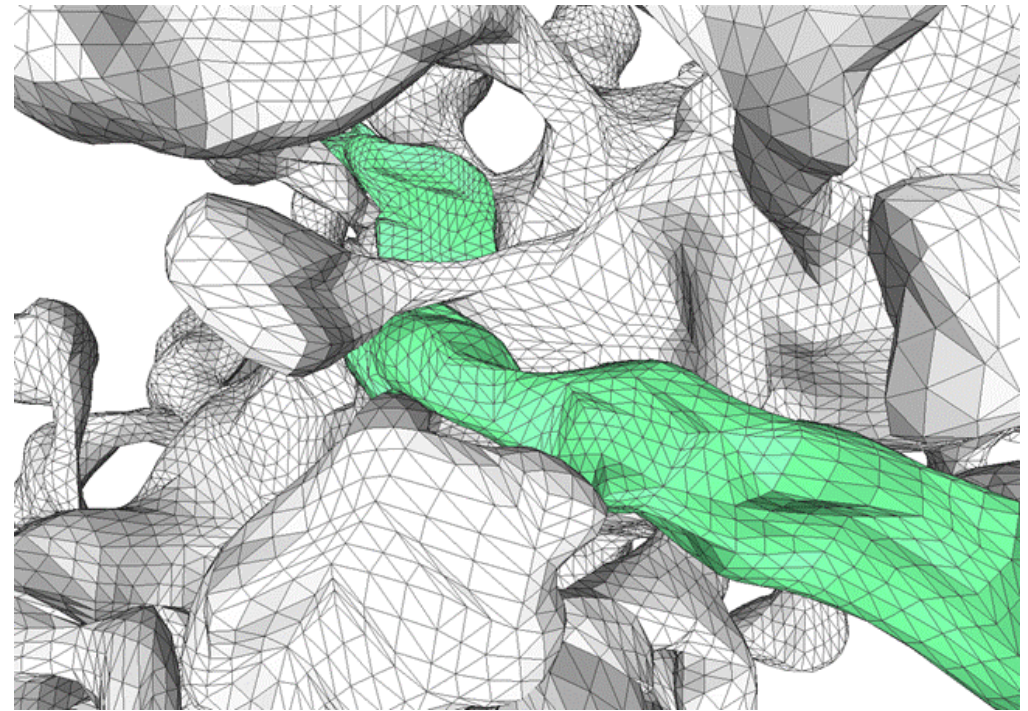


Computational Visualization Center (CVC) <http://cvcweb.ices.utexas.edu>
Dept. of Computer Science / Institute for Computational Engineering and Sciences
University of Texas at Austin

Mesh Quality Improvement



(a)



(b)



1. Tri/Tetra Quality Improvement Metrics

- Criteria:
 - Triangle: the aspect ratio = inscribed sphere radius / circumsphere radius
 - Edge-ratio
 - Tetrahedron:
 - Joe-Liu parameter
 - Minimum volume bound

- **Joe-Liu parameter:** Let $|s|$ denote the volume (which may be negative) of a given d -simplex ' s ', $v_i (i = 0, \dots, d)$ denote the vertices of s , and e_{ij} denote the edges of s that connect v_i to v_j . We compute the Joe-Liu parameter of a d -simplex s as:

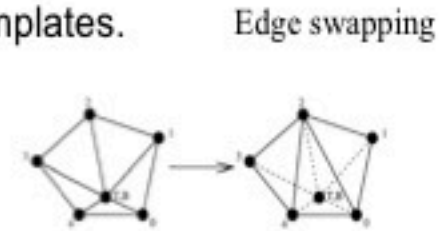
$$F(s, d) = \frac{f(s, d)}{g(s, d)} = \frac{2^{2(1-\frac{1}{d})} \times 3^{\frac{d-1}{2}} \times |s|^{\frac{2}{d}}}{\sum_{0 \leq i < j \leq d} |e_{ij}|^2} \quad (6)$$

For tetrahedral meshes, d is set to be 3. $F(s, 3)$ is normalized to yield maximal value of 1 for the unit tetrahedron (with volume 1/6).

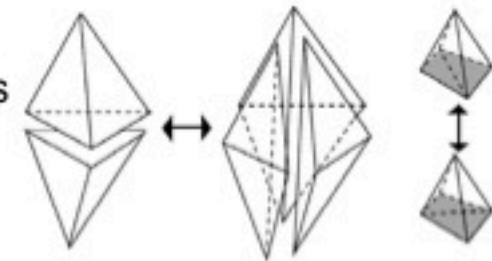


2. Tri/Tetra Quality Improvement Schemes

- Local refinement/coarsening – inserting/deleting vertices
 - refinement: edge bisection (Rivara 1997, Bajaj 1996), point insertion and templates.
 - coarsening: edge contraction
- Local remeshing - face/edge swapping (Freitag 1997)
- Mesh smoothing - relocating vertices



- Averaging methods
 - Laplacian smoothing (Field 1988): replace the node with the average of its neighbors.
 - Constrained/weighted Laplacian smoothing (Canann 1998, Bajaj 2002)
- Optimization-based methods (Canann 1998, Freitag 1995, 1997)
 - It measures the quality of the surrounding elements to a node, and attempt to optimize by computing the local gradient of the element quality w.r.t. the node location. The node moves along the increasing gradient direction until an optimum is reached.
 - Combined Laplacian/optimization-based approach
- Physically-based methods
 - Lohner (1986) simulates the force between neighboring nodes as a system of spring.
 - Shimada (1997) and Bossen (1996) view the nodes as the center of bubbles that are repositioned to attain equilibrium. Anisotropic meshes can be achieved.



Face swapping



Quality Improvement with Surface Diffusion Flow

- Nonlinear geometric PDEs have been used to efficiently solve surface modeling problems: surface blending, N-sided filling and free-form surface fitting [1][2]. These nonlinear equations are discretized based on discrete differential geometry operators.

$$\frac{\partial x}{\partial t} = V_n(k_1, k_2, x)N(x), \quad M(0) = M_0.$$

Where $X(t)$ – a surface point on a closed surface $M(t)$

$V_n(k_1, K_2, x)$ – the normal velocity of $M(t)$

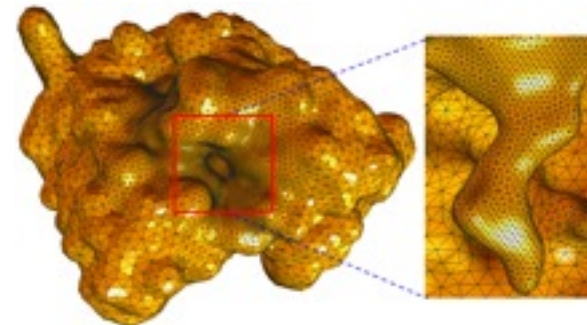
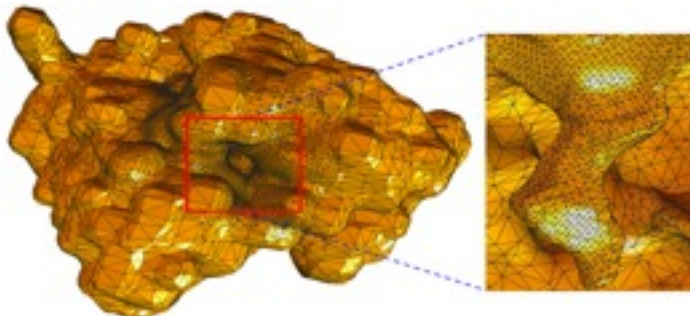
$N(x)$ – the unit normal of the surface at $x(t)$

- Mean Curvature Flow: $V_n = -H = -(k_1 + k_2)/2$
- Average Mean Curvature Flow: $V_n = h(t) - H(t)$

$$\text{where } h(t) = \int_{M(t)} H d\sigma / \int_{M(t)} d\sigma$$

- Surface Diffusion Flow: $V_n = \Delta H$

- High Order Flow: $\frac{\partial x}{\partial t} = (-1)^{k+1} \Delta^k H N(x)$



- Discretized Laplace-Beltrami operator over triangles [1][3]

$$\Delta f(p_i) = \frac{1}{A(p_i)} \sum_{j \in N_1(i)} \frac{\cot \alpha_{ij} + \cot \beta_{ij}}{2} [f(p_j) - f(p_i)],$$

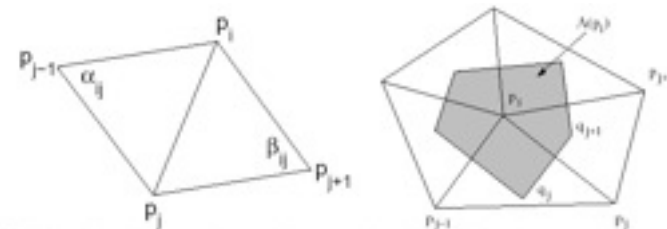


Fig 3.1: Left: The definition of the angles α_{ij} and β_{ij} . Right: The definition of the area $A(p_i)$.

$$H(p_i)N(p_i) = \frac{1}{2A(p_i)} \sum_{j \in N_1(i)} \frac{\cot \alpha_{ij} + \cot \beta_{ij}}{2} (p_i - p_j)$$

$$\Delta^k f(p_i) = \Delta(\Delta^{k-1} f)(p_i) = \frac{1}{A(p_i)} \sum_{j \in N_1(i)} \frac{\cot \alpha_{ij} + \cot \beta_{ij}}{2} [\Delta^{k-1} f(p_j) - \Delta^{k-1} f(p_i)]$$

Xu G., Pan Q., Bajaj C. **Discrete Surface Modeling using Geometric Flows.** *Computer Aided Geometric Design*, 2006.



Computational Visualization Center (CVC) <http://cvcweb.ices.utexas.edu>
 Dept. of Computer Science / Institute for Computational Engineering and Sciences
 University of Texas at Austin

Surface Diffusion Flow Properties

1. Vertex normal movement:

- The surface diffusion flow preserves volume
- The surface diffusion flow preserves a sphere accurately if the initial mesh is close to a sphere.

2. Vertex tangent movement:

- The tangent movement doesn't change the surface shape
- Area-weighted averaging method, suitable for adaptive meshes.



Quality Metrics for Hex (Quads)

- Three error metrics [Kober et. al. 2000] [Knupp 2000] [Oddy et. al. 1988]

Edge vector $e_i = x_i - x$, $i = 1, \dots, m$

Jacobian matrix $J = [e_1 e_2 \dots e_m]$

The condition number $\kappa(J) = |J| |J^{-1}|$

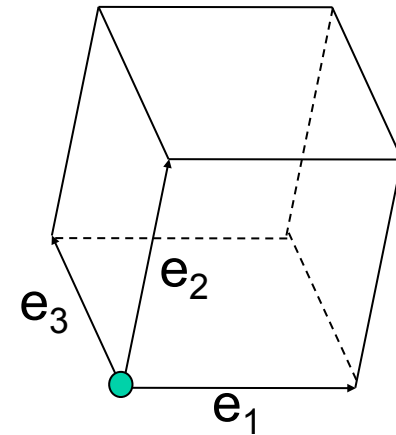
$$|J| = (\text{tr}(J^T J))^{1/2} \quad |J^{-1}| = \frac{|J|}{\det(J)}$$

Where

$$\text{Jacobian}(x) = \det(J) = \sqrt{\det(J^T J)} \quad (1)$$

$$\kappa(x) = \frac{1}{m} |J^{-1}| |J| \quad (2)$$

$$\text{Oddy}(x) = \frac{(|J^T J|^2 - \frac{1}{m} |J|^4)}{\det(J)^{\frac{4}{m}}} \quad (3)$$



- Set the condition number as the objective function, and use the conjugate gradient method to find an optimized position for a node with the worst condition number.



Quadrilateral Surface Mesh Improvement

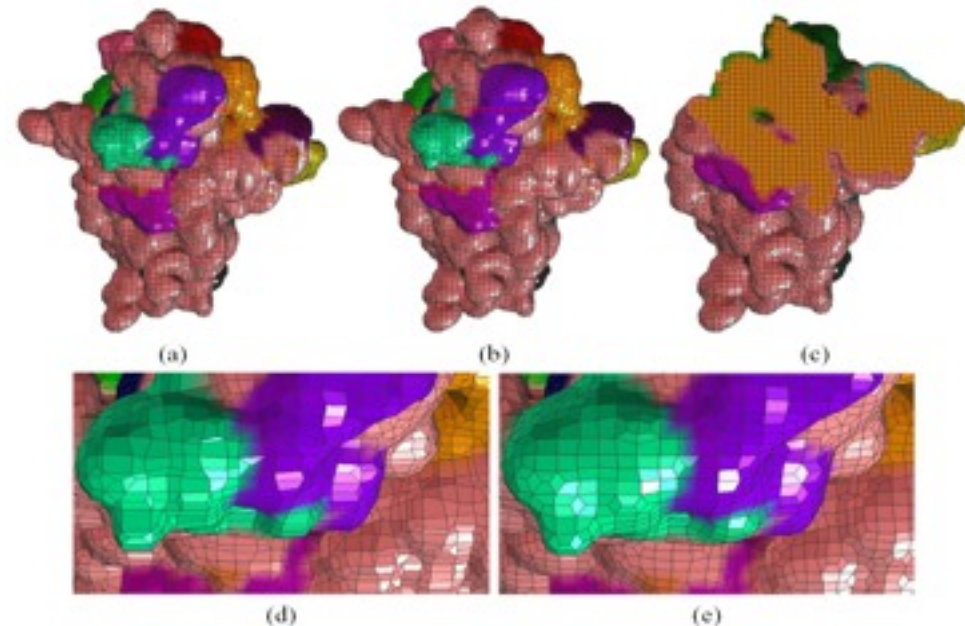
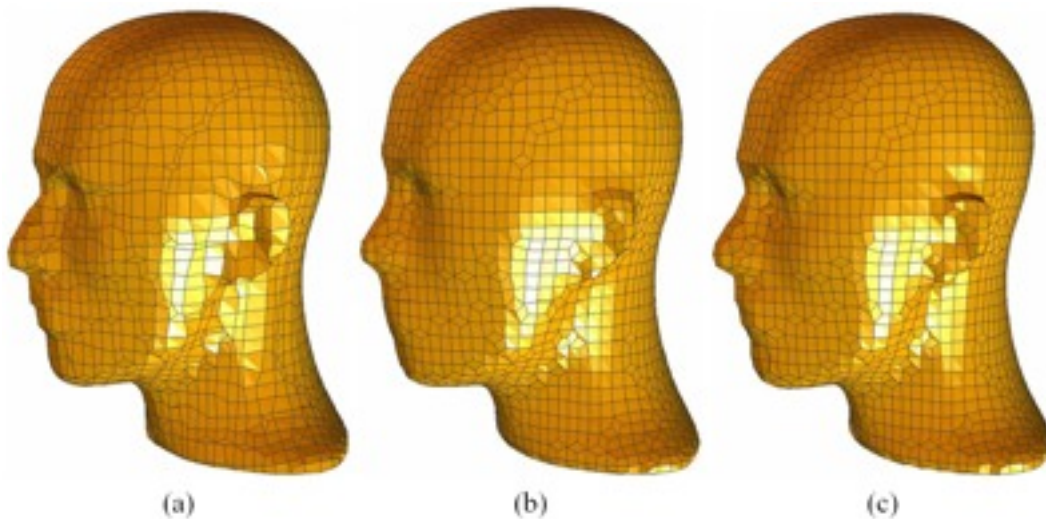
- Surface diffusion geometric flow

$$\frac{\partial x}{\partial t} = \Delta H(x) \mathbf{n}(x)$$

where Δ - the Laplace-Beltrami (LB) operator

H - the mean curvature

$\mathbf{n}(x)$ - the unit normal vector at the node x .



Quad Area Calculation

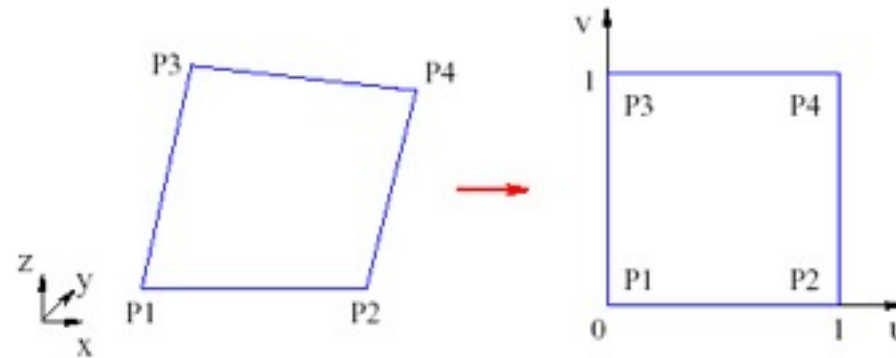


Fig. 2. A quad $[p_1 p_2 p_4 p_3]$ is mapped into a bilinear parametric surface.

$$S(u, v) = (1 - u)(1 - v)p_1 + u(1 - v)p_2 + (1 - u)v p_3 + u v p_4.$$

The tangents:

$$S_u(u, v) = (1 - v)(p_2 - p_1) + v(p_4 - p_3),$$

$$S_v(u, v) = (1 - u)(p_3 - p_1) + u(p_4 - p_2).$$

The area:

$$A = \int_0^1 \int_0^1 \sqrt{\|S_u \times S_v\|^2} dudv = \int_0^1 \int_0^1 \sqrt{\|S_u\|^2 \|S_v\|^2 - (S_u, S_v)^2} dudv.$$

Four-point Gaussian quadrature rule:

$$\int_0^1 \int_0^1 f(u, v) dudv \approx \frac{f(q_1) + f(q_2) + f(q_3) + f(q_4)}{4}$$

$$q^- = \frac{1}{2} - \frac{\sqrt{3}}{6}, \quad q^+ = \frac{1}{2} + \frac{\sqrt{3}}{6},$$

$$q_1 = (q^-, q^-), \quad q_2 = (q^+, q^-),$$

$$q_3 = (q^-, q^+), \quad q_4 = (q^+, q^+).$$



Discretized Laplace-Beltrami Operator (I)

$$\lim_{diam(R) \rightarrow 0} \frac{2\nabla A}{A} = \mathbf{H}(p)$$

where A is the area of a region R over the surface around the surface point p , $diam(R)$ denotes the diameter of the region R , and $\mathbf{H}(p)$ is the mean curvature normal.

$$\begin{aligned} \nabla A &= \int_0^1 \int_0^1 \nabla \sqrt{\|S_u\|^2 \|S_v\|^2 - (S_u, S_v)^2} dudv \\ &= \int_0^1 \int_0^1 \frac{S_u(S_v, (v-1)S_v - (u-1)S_u)}{\sqrt{\|S_u\|^2 \|S_v\|^2 - (S_u, S_v)^2}} dudv \\ &\quad + \int_0^1 \int_0^1 \frac{S_v(S_u, (u-1)S_u - (v-1)S_v)}{\sqrt{\|S_u\|^2 \|S_v\|^2 - (S_u, S_v)^2}} dudv \\ &= \alpha_{21}(p_2 - p_1) + \alpha_{43}(p_4 - p_3) \\ &\quad + \alpha_{31}(p_3 - p_1) + \alpha_{42}(p_4 - p_2), \end{aligned}$$

$$\alpha_1 = -\alpha_{21} - \alpha_{31}, \quad \alpha_2 = -\alpha_{21} + \alpha_{42},$$

$$\alpha_3 = \alpha_{31} - \alpha_{43}, \quad \alpha_4 = \alpha_{43} + \alpha_{42}.$$

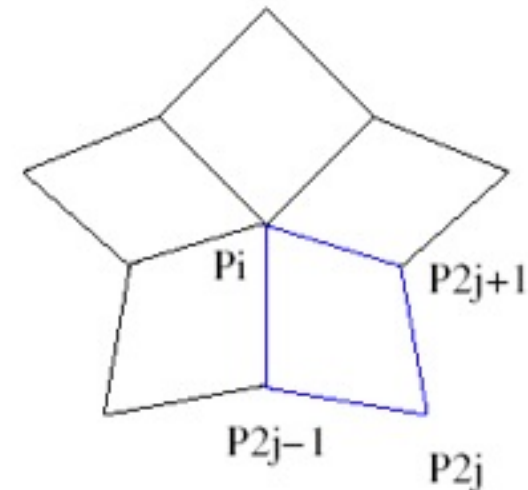
$$\nabla A = \alpha_1 p_1 + \alpha_2 p_2 + \alpha_3 p_3 + \alpha_4 p_4$$

$$= \alpha_2(p_2 - p_1) + \alpha_3(p_3 - p_1) + \alpha_4(p_4 - p_1).$$



Discretized Laplace-Beltrami Operator (II)

$$\begin{aligned} \mathbf{H}(p_i) &\approx \frac{2}{A(p_i)} \sum_{j=1}^n [\alpha_j^i (p_{2j-1} - p_i) \\ &\quad + \beta_j^i (p_{2j+1} - p_i) + \gamma_{j+1}^i (p_{2j} - p_i)] \\ &= \sum_{k=1}^{2n} w_k^i (p_k - p_i) \end{aligned}$$



$$w_{2j}^i = \frac{2\gamma_j^i}{A(p_i)}, \quad w_{2j-1}^i = \frac{2(\alpha_j^i + \beta_{j-1}^i)}{A(p_i)}, \quad w_{2j+1}^i = \frac{2(\alpha_{j+1}^i + \beta_j^i)}{A(p_i)}.$$

Using the relation $\Delta x = 2H(p_i)$

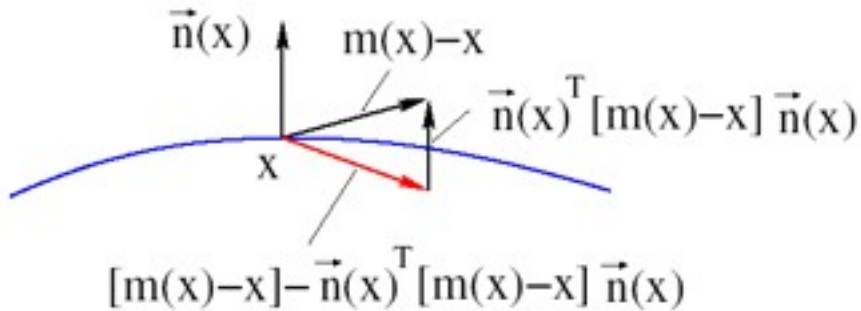
$$\Delta f(p_i) \approx 2 \sum_{k=1}^{2n} w_k^i (f(p_k) - f(p_i)).$$

$$\begin{aligned} \Delta H(p_i) \mathbf{n}(p_i) &\approx 2 \sum_{k=1}^{2n} w_k^i (H(p_k) - H(p_i)) \mathbf{n}(p_i) \\ &= 2 \sum_{k=1}^{2n} w_k^i \left[\mathbf{n}(p_i) \mathbf{n}(p_k)^T \mathbf{H}(p_k) - \mathbf{H}(p_i) \right] \end{aligned}$$



Tangent Movement

$$\frac{\partial x}{\partial t} = \Delta H(x) \mathbf{n}(x) + v(x) \mathbf{T}(x)$$



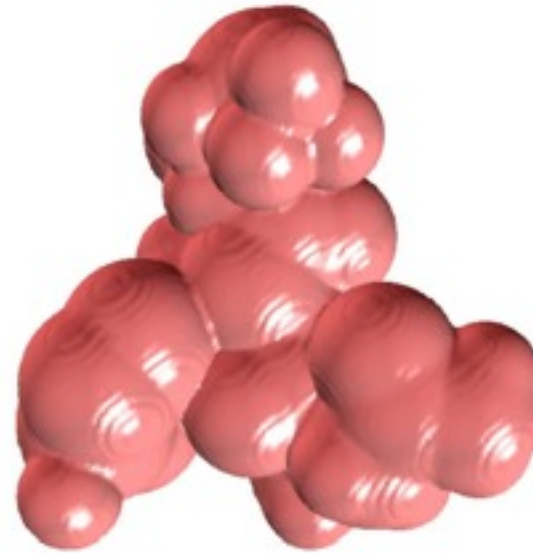
Mass center:

$$\int_S \|y - p\|^2 d\sigma = \min.$$

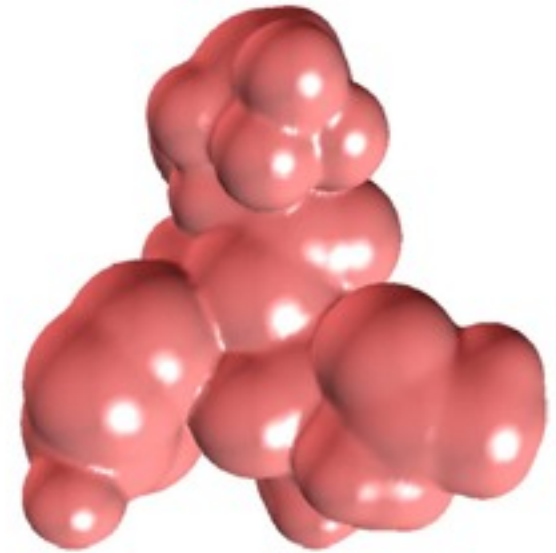
$$m(p_i) = \sum_{j=1}^n \left(\frac{p_i + p_{2j-1} + p_{2j} + p_{2j+1}}{4} A_j \right) / A_{total}^i$$

Temporal discretization:

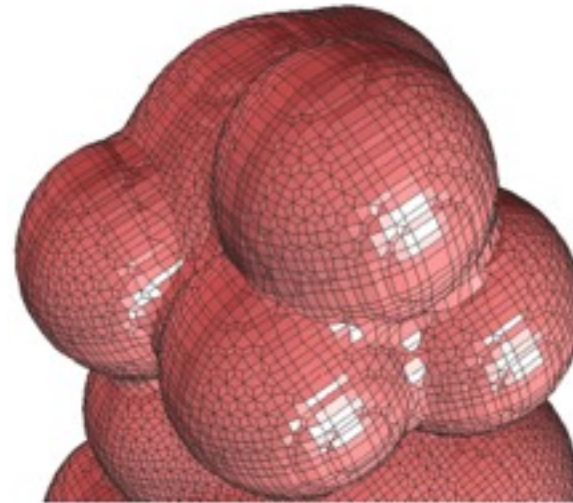
- semi-implicit Euler scheme
- conjugate gradient iterative method



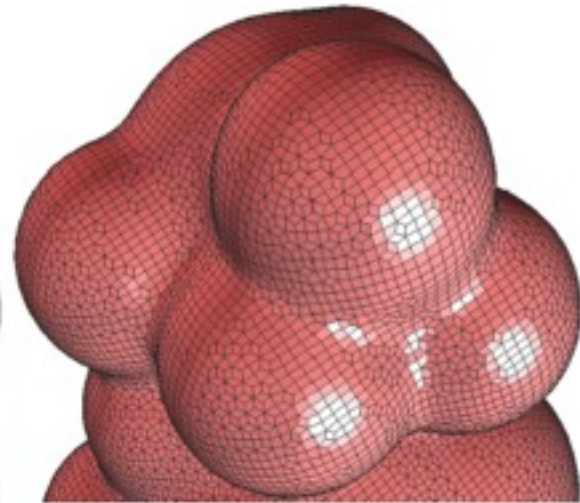
(a)



(b)



(c)



(d)



Hexahedral Volumetric Mesh

- Surface Vertex Movement
- Interior Vertex Movement

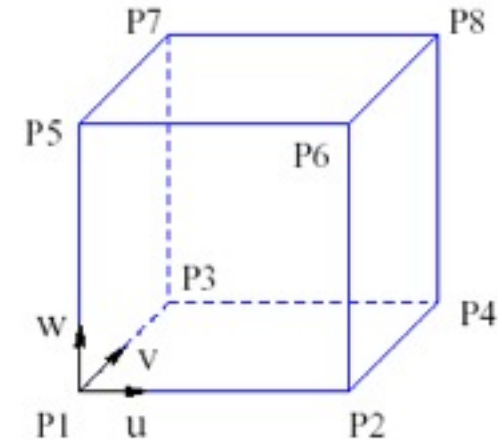
$$\begin{aligned}
 V(u, v, w) &= (1-u)(1-v)(1-w)p_1 \\
 &+ u(1-v)(1-w)p_2 + (1-u)v(1-w)p_3 \\
 &+ uv(1-w)p_4 + (1-u)(1-v)wp_5 \\
 &+ u(1-v)wp_6 + (1-u)vwp_7 \\
 &+ uvwp_8.
 \end{aligned}$$

$$\begin{aligned}
 V_u(u, v, w) &= (1-v)(1-w)(p_2 - p_1) + v(1-w)(p_4 - p_3) \\
 &+ (1-v)w(p_6 - p_5) + vw(p_8 - p_7),
 \end{aligned}$$

$$\begin{aligned}
 V_v(u, v, w) &= (1-u)(1-w)(p_3 - p_1) + u(1-w)(p_4 - p_2) \\
 &+ (1-u)w(p_7 - p_5) + uw(p_8 - p_6),
 \end{aligned}$$

$$\begin{aligned}
 V_w(u, v, w) &= (1-u)(1-v)(p_5 - p_1) + u(1-v)(p_6 - p_2) \\
 &+ (1-u)v(p_7 - p_3) + uv(p_8 - p_4).
 \end{aligned}$$

$$V = \int_0^1 \int_0^1 \int_0^1 \sqrt{\bar{V}} \, dudvdw \quad \bar{V} = \| (V_u \times V_v) \cdot V_w \|^2$$



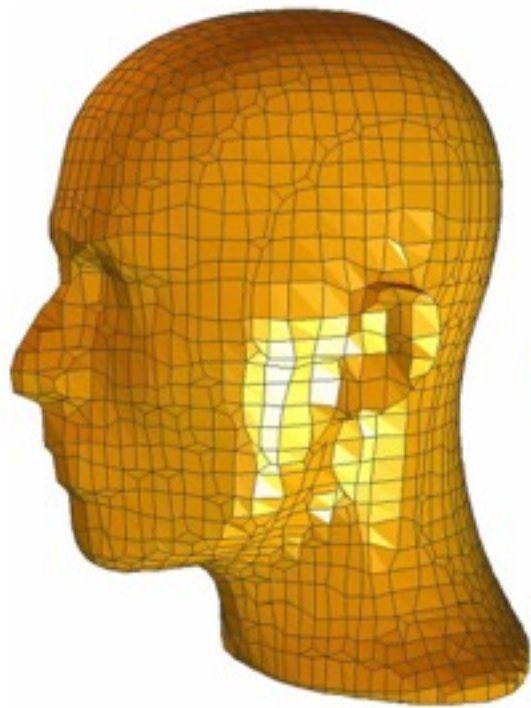
$$\int_0^1 \int_0^1 \int_0^1 f(u, v, w) \, dudvdw \approx \frac{\sum_{j=1}^8 f(q_j)}{8},$$

$$q^- = \frac{1}{2} - \frac{\sqrt{3}}{6}, \quad q^+ = \frac{1}{2} + \frac{\sqrt{3}}{6},$$

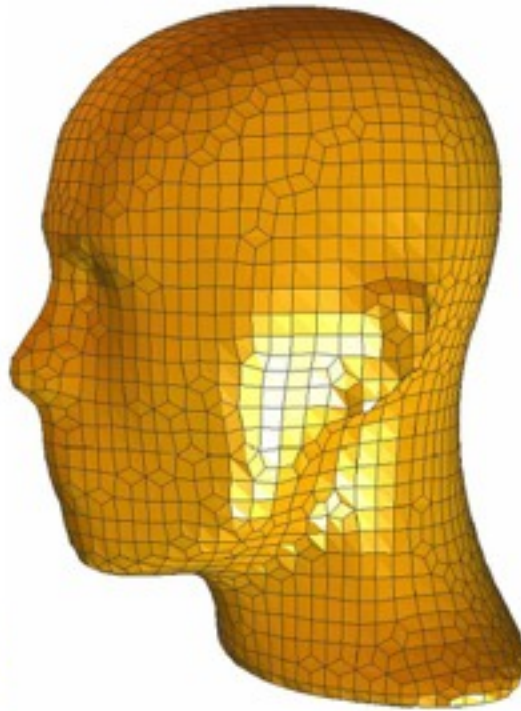
$$\begin{aligned}
 q_1 &= (q^-, q^-, q^-), & q_2 &= (q^+, q^-, q^-), \\
 q_3 &= (q^-, q^+, q^-), & q_4 &= (q^+, q^+, q^-), \\
 q_5 &= (q^-, q^-, q^+), & q_6 &= (q^+, q^-, q^+), \\
 q_7 &= (q^-, q^+, q^+), & q_8 &= (q^+, q^+, q^+).
 \end{aligned}$$

$$m(p_i) = \sum_{j \in N(i)} \left(\frac{1}{8} \sum_{j=1}^8 p_j V_j \right) / V_{total}^i,$$

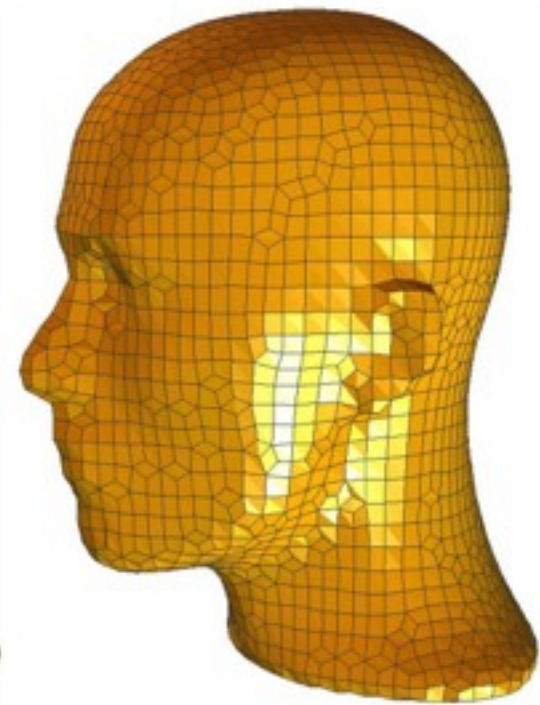




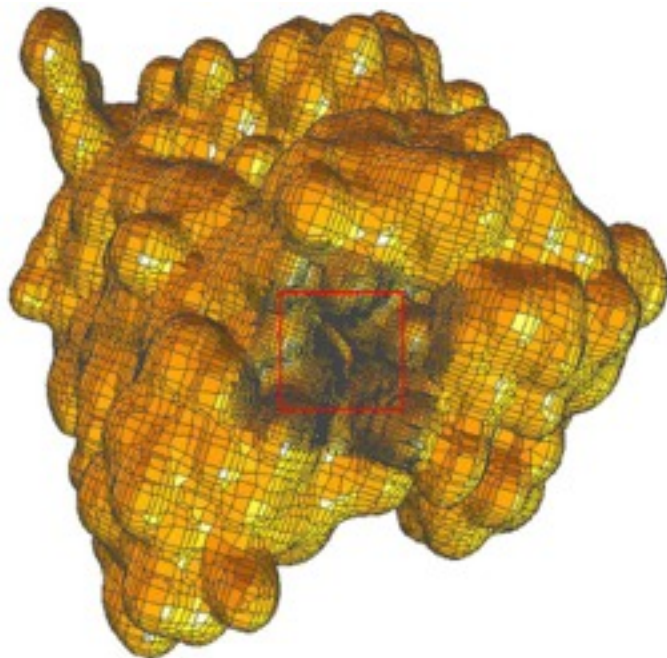
(a)



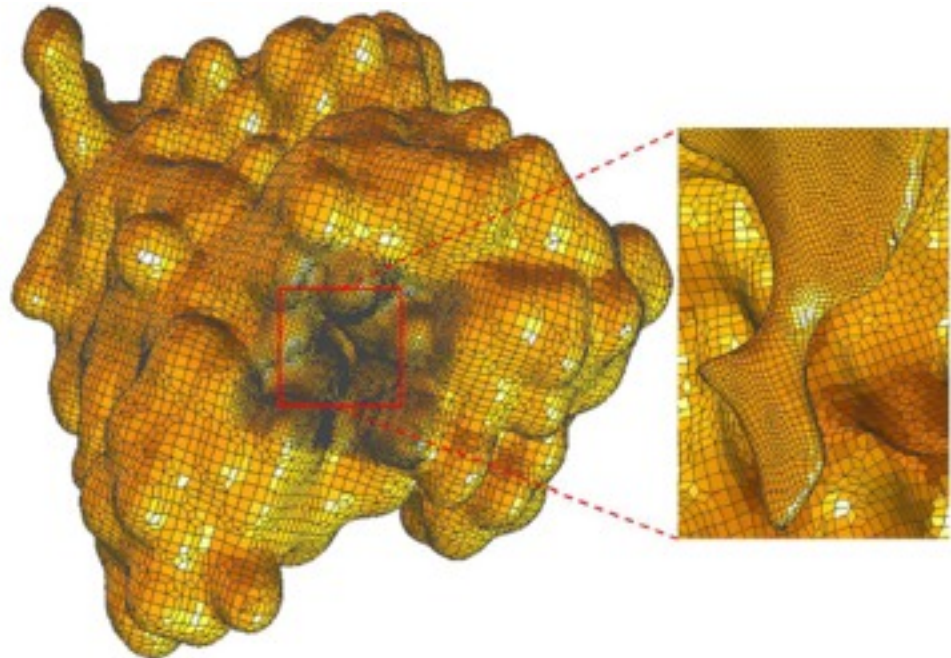
(b)



(c)



(a)



(b)



References

J. Edwards and C. Bajaj

Topologically correct reconstruction of tortuous contour forests

Computer-Aided Design, 43(10): 1296-1306, 2011, NIHMSID 319941, [doi:10.1016/j.cad.2011.06.019](https://doi.org/10.1016/j.cad.2011.06.019), [PMID: 22003256](https://pubmed.ncbi.nlm.nih.gov/22003256/), *PMC Journal in Process*.

Y. Zhang, T. J.R. Hughes, C. Bajaj

An Automatic 3D Mesh Generation Method for Domains with Multiple Materials.

Computer Methods in Applied Mechanics and Engineering (CMAME), 199(5-8): 405-415, Jan 2009, NIHMSID: 132380, *Publ.ID: CMA8983*, [doi:10.1016/j.cma.2009.06.007](https://doi.org/10.1016/j.cma.2009.06.007), [PMCID: PMC2805160](https://pubmed.ncbi.nlm.nih.gov/PMC2805160/).

Y. Zhang, C. Bajaj, G. Xu

Surface Smoothing and Quality Improvement of Quadrilateral/Hexahedral Meshes using Geometric Flow

Comm. in Numerical Methods in Engineering, Vol. 24, 2008. [doi: 10.1002/cnm.1067](https://doi.org/10.1002/cnm.1067), [PMCID: PMC2761001](https://pubmed.ncbi.nlm.nih.gov/PMC2761001/).

Y. Zhang, C. Bajaj

Adaptive and Quality Quadrilateral/Hexahedral Meshing from Volumetric Data

Computer Methods in Applied Mechanics and Engineering, Volume 195, Issues 9-12, 1 February 2006, Pages 942-960, [doi:10.1016/j.cma.2005.02.016](https://doi.org/10.1016/j.cma.2005.02.016), [PMCID: PMC2740490](https://pubmed.ncbi.nlm.nih.gov/PMC2740490/) ([Related CVC Project](#))

G. Xu, Q. Pan, C. Bajaj

Discrete Surface Modeling Using Partial Differential Equations

Computer Aided Geometric Design, Volume 23/2, pp 125-145, 2006, [doi:10.1016/j.cagd.2005.05.004](https://doi.org/10.1016/j.cagd.2005.05.004), [PMCID: PMC2760856](https://pubmed.ncbi.nlm.nih.gov/PMC2760856/)

Y. Zhang, G. Xu, C. Bajaj

Quality Meshing of Implicit Solvation Models of Biomolecular Structures

The special issue of Computer Aided Geometric Design (CAGD) on Applications of Geometric Modeling in the Life Sciences, Volume 23, Issue 6, August 2006, Pages 510-530, [doi: 10.1016/j.cagd.2006.01.008](https://doi.org/10.1016/j.cagd.2006.01.008), [PMCID: PMC2756697](https://pubmed.ncbi.nlm.nih.gov/PMC2756697/)

Y. Zhang, C. Bajaj, B. Sohn

3D Finite Element Meshing from Imaging Data

Computer Methods in Applied Mechanics and Engineering (CMAME) on Unstructured Mesh Generation, 194, 48-49, 5083-5106, 2005, [doi:10.1016/j.cma.2004.11.026](https://doi.org/10.1016/j.cma.2004.11.026), [PMCID: PMC2748876](https://pubmed.ncbi.nlm.nih.gov/PMC2748876/).

Adaptive and Quality Quadrilateral/Hexahedral Meshing from Volumetric Imaging Data

In Proceedings of 13th International Meshing Roundtable, pp. 365-376. Willamsburg, VA. September 19-22, 2004. ([pdf](#))

References (contd)

C. Bajaj, E. Coyle, K. Lin

Arbitrary Topology Shape Reconstruction from Planar Cross Sections

Graphical Models and Image Processing, 58:6, (1996), 524-543. ([pdf](#))

C. Bajaj, T. Dey

Convex Decomposition of Polyhedra and Robustness

Siam Journal on Computing, 21, 2, (1992), 339-364. ([pdf](#))

T. Dey, K. Sugihara, C. Bajaj

Delaunay Triangulations in Three Dimensions with Finite Precision Arithmetic

Computer Aided Geometric Design, 9:6(1992), 457-470. ([pdf](#))

T. Dey, C. Bajaj, K. Sugihara

On Good Triangulations in Three Dimensions

International Journal of Computational Geometry and Applications, 2, 1, (1992), 75-95. ([pdf](#))

C. Bajaj

A Laguerre Voronoi Based Scheme for Meshing Particle Systems

Japan Journal of Industrial and Applied Mathematics, (JJIAM), vol. 22, No. 2, Pages 167-177, June 2005, [doi: 10.1007/BF03167436](https://doi.org/10.1007/BF03167436), [PMCID: PMC2865151](https://pubmed.ncbi.nlm.nih.gov/2865151/).

Y. Zhang, G. Xu, C. Bajaj,

Surface Smoothing and Quality Improvement of Quadrilateral/Hexahedral Meshes with Geometric Flow

Comm. in Numerical Methods in Engineering, Vol. 24, 2008. [doi:10.1002/cnm.1067](https://doi.org/10.1002/cnm.1067), [PMCID: PMC2761001](https://pubmed.ncbi.nlm.nih.gov/2761001/).

C. Bajaj, G. Xu

Anisotropic Diffusion of Surfaces and Functions on Surfaces

ACM Transactions on Graphics, 22, 1, (2003), 4-32, [doi: 10.1145/588272.588276](https://doi.org/10.1145/588272.588276) ([pdf](#))

C. Bajaj, S. Schaefer, J. Warren, G. Xu

A Subdivision Scheme for Hexahedral Meshes

The Visual Computer, Vol. 18. Numbers 5-6. Pages 343-356. August 2002, [doi: 10.1007/s003710100150](https://doi.org/10.1007/s003710100150).([pdf](#))

C. Bajaj, E. Coyle, K. Lin

Tetrahedral Meshes from Planar Cross Sections

Computer Methods in Applied Mechanics and Engineering, Vol. 179 (1999), pp. 31-52. ([pdf](#)) ([ps](#))